Immunity, Volume *54*

Supplemental information

Global analysis of shared T cell specificities in human non-small cell lung cancer enables HLA inference and antigen discovery

Shin-Heng Chiou, Diane Tseng, Alexandre Reuben, Vamsee Mallajosyula, Irene S. Molina, Stephanie Conley, Julie Wilhelmy, Alana M. McSween, Xinbo Yang, Daisuke Nishimiya, Rahul Sinha, Barzin Y. Nabet, Chunlin Wang, Joseph B. Shrager, Mark F. Berry, Leah Backhus, Natalie S. Lui, Heather A. Wakelee, Joel W. Neal, Sukhmani K. Padda, Gerald J. Berry, Alberto Delaidelli, Poul H. Sorensen, Elena Sotillo, Patrick Tran, Jalen A. Benson, Rebecca Richards, Louai Labanieh, Dorota D. Klysz, David M. Louis, Steven A. Feldman, Maximilian Diehn, Irving L. Weissman, Jianjun Zhang, Ignacio I. Wistuba, P. Andrew Futreal, John V. Heymach, K. Christopher Garcia, Crystal L. Mackall, and Mark M. Davis

Figure S1

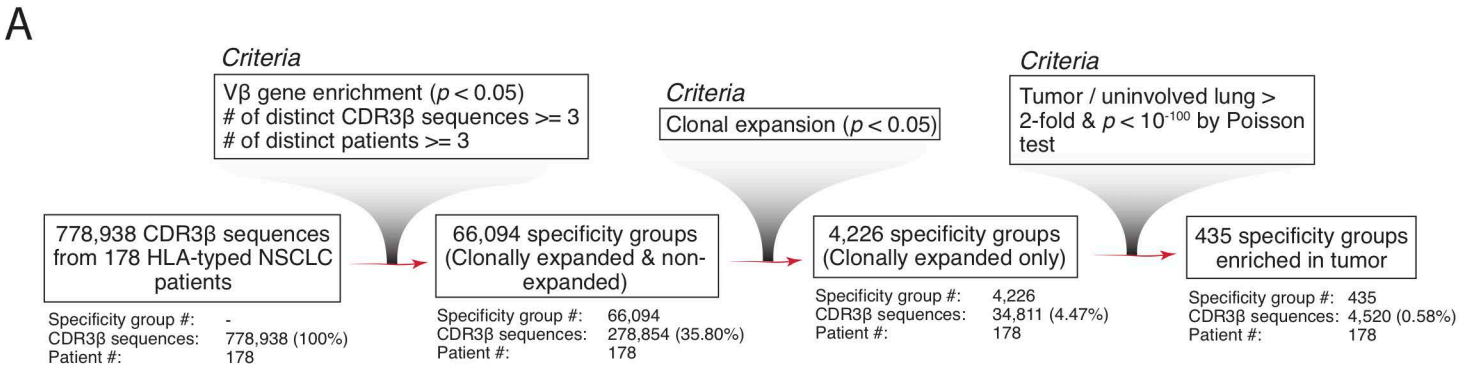
A
Criteria
Vβ gene enrichment (p < 0.05)
# of distinct CDR3β sequences >= 3
# of distinct patients >= 3
Criteria
Clonal expansion (p < 0.05)
Criteria
Tumor / uninvolved lung > 2-fold & p < 10-100 by Poisson test
778,938 CDR3β sequences from 178 HLA-typed NSCLC patients
Specificity group #: -
CDR3β sequences: 778,938 (100%)
Patient #: 178
66,094 specificity groups (Clonally expanded & non-expanded)
Specificity group #: 66,094
CDR3β sequences: 278,854 (35.80%)
Patient #: 178
4,226 specificity groups (Clonally expanded only)
Specificity group #: 4,226
CDR3β sequences: 34,811 (4.47%)
Patient #: 178
435 specificity groups enriched in tumor
Specificity group #: 435
CDR3β sequences: 4,520 (0.58%)
Patient #: 178

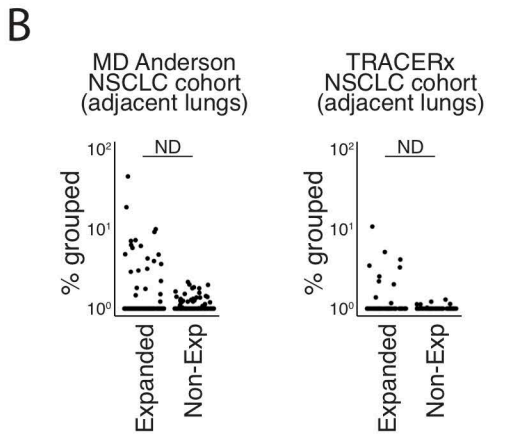
B
MD Anderson NSCLC cohort (adjacent lungs)
TRACERx NSCLC cohort (adjacent lungs)
ND
% grouped
Expanded
Non-Exp

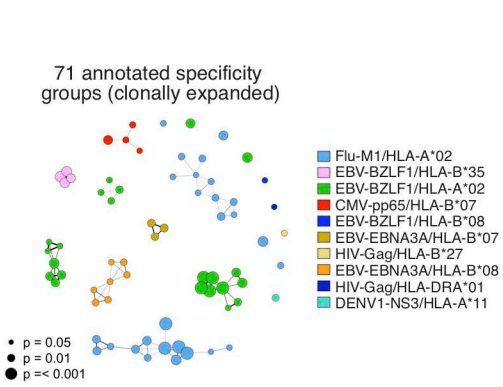
C
71 annotated specificity groups (clonally expanded)
Flu-M1/HLA-A*02
EBV-BZLF1/HLA-B*35
EBV-BZLF1/HLA-A*02
CMV-pp65/HLA-B*07
EBV-BZLF1/HLA-B*08
EBV-EBNA3A/HLA-B*07
HIV-Gag/HLA-B*27
EBV-EBNA3A/HLA-B*08
HIV-Gag/HLA-DRA*01
DENV1-NS3/HLA-A*11
p = 0.05
p = 0.01
p =< 0.001

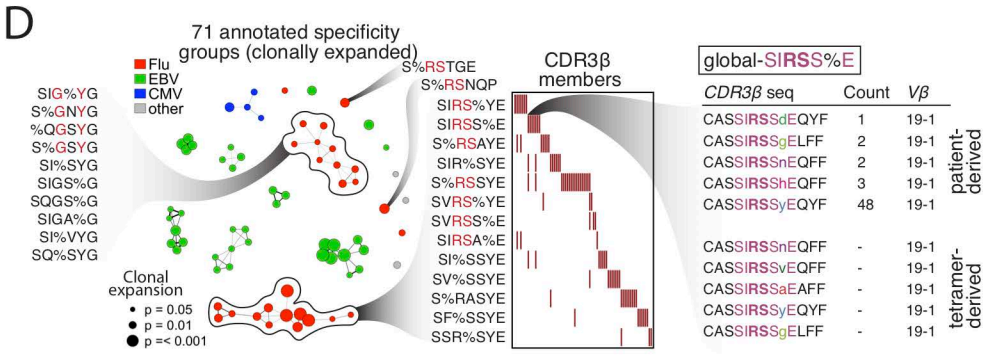
D
71 annotated specificity groups (clonally expanded)
Flu
EBV
CMV
other
SIG%YG
S%GNYG
%QGSYG
S%GSYG
SI%SYG
SIGS%G
SQGS%G
SIGA%G
SI%VYG
SQ%SYG
Clonal expansion
p = 0.05
p = 0.01
p =< 0.001
S%RSTGE
S%RSNQP
SIRS%YE
SIRSS%E
S%RSAYE
SIR%SYE
S%RSSYE
SVRS%YE
SVRSS%E
SIRSA%E
SI%SSYE
SV%SSYE
S%RASYE
SF%SSYE
SSR%SYE
CDR3β members
global-SIRSS%E
CDR3β seq
Count
Vβ
CASSIRSSdEQYF 1 19-1
CASSIRSSgELFF 2 19-1
CASSIRSSnEQFF 2 19-1
CASSIRSShEQFF 3 19-1
CASSIRSSyEQYF 48 19-1
patient-derived
CASSIRSSnEQFF - 19-1
CASSIRSSvEQFF - 19-1
CASSIRSSaEAFF - 19-1
CASSIRSSyEQYF - 19-1
CASSIRSSgELFF - 19-1
tetramer-derived

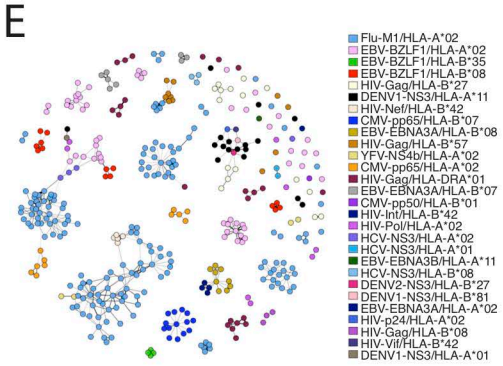
E
Flu-M1/HLA-A*02
EBV-BZLF1/HLA-A*02
EBV-BZLF1/HLA-B*35
EBV-BZLF1/HLA-B*08
HIV-Gag/HLA-B*27
DENV1-NS3/HLA-A*11
HIV-Nef/HLA-B*42
CMV-pp65/HLA-B*07
EBV-EBNA3A/HLA-B*08
HIV-Gag/HLA-B*57
YFV-NS4b/HLA-A*02
CMV-pp65/HLA-A*02
HIV-Gag/HLA-DRA*01
EBV-EBNA3A/HLA-B*07
CMV-pp50/HLA-B*01
HIV-Int/HLA-B*42
HIV-Pol/HLA-A*02
HCV-NS3/HLA-A*02
HCV-NS3/HLA-A*01
EBV-EBNA3B/HLA-A*11
HCV-NS3/HLA-B*08
DENV2-NS3/HLA-B*27
DENV1-NS3/HLA-B*81
EBV-EBNA3A/HLA-A*02
HIV-p24/HLA-A*02
HIV-Gag/HLA-B*08
HIV-Vif/HLA-B*42
DENV1-NS3/HLA-A*01

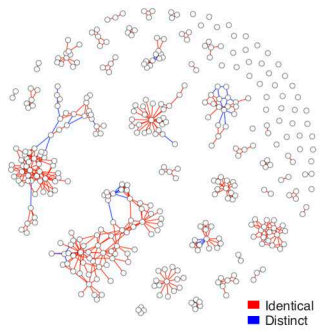
F
Identical
Distinct

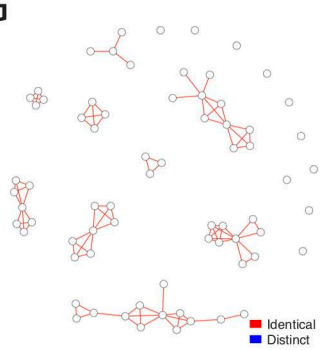
G
Identical
Distinct

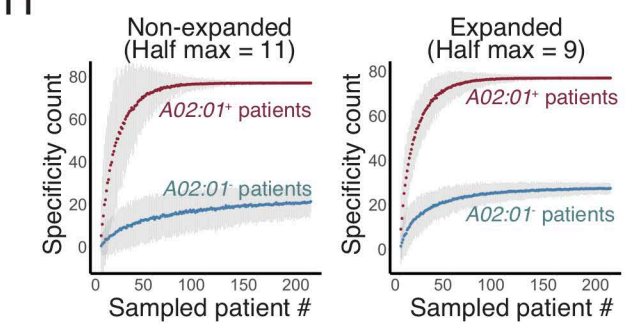
H
Non-expanded (Half max = 11)
Expanded (Half max = 9)
A02:01+ patients
A02:01- patients
Specificity count
Sampled patient #

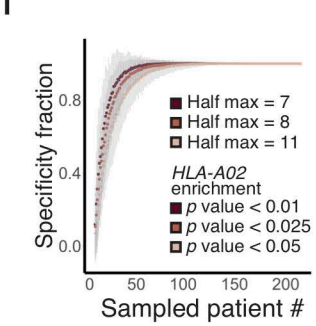
I
Specificity fraction
Half max = 7
Half max = 8
Half max = 11
HLA-A02 enrichment
p value < 0.01
p value < 0.025
p value < 0.05
Sampled patient #

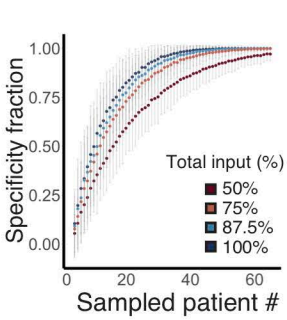
J
Specificity fraction
Total input (%)
50%
75%
87.5%
100%
Sampled patient #

Figure S1, related to Figure 1

(**A**) Specificity inference pipeline. (**B**) Low percentages of TCR clonotypes from adjacent lung tissues are grouped into tumor-enriched specificity groups. The percentages of the top 20 most expanded CDR3β clonotypes from the adjacent lung tissues of patients belonging to the MDACC NSCLC cohort (n=178 samples, left) and the TRACERx cohort (n=63 samples, right) were quantified for those that belonged to the 435 tumor-enriched specificity groups as in Figure 1B (% grouped, $\log_{10}$-converted). The same analysis was performed on the remainder of the CDR3β clonotypes (Non-exp, non-expanded). ND, no statistically significant difference was found. (**C**) The 71 clonally expanded specificity groups annotated and colored with 10 indicated tetramers are shown in the network. (**D**) Left to right, network analysis of 71 clonally expanded specificity groups colored as in Figure 1C is shown; two large Flu-related communities (red) are circled and the CDR3β members of the specificity groups are highlighted with the previously reported short motifs "RS" and "GxY" highlighted in red font; heatmap showing distinct CDR3β members (columns) of the Flu-related (with the "RS" motif) specificity groups (rows) and the levels of shared CDR3β members between specificity groups within the circled community; table showing an example of the "SIRSS%E" specificity group containing the short "RS" motif (bold) that is annotated with 5 Flu-specific tetramer sequences (bottom). The counts of distinct CDR3β members from tumor and the *Vβ* gene usage are shown (top). (**E**) 394 specificity groups annotated with indicated tetramers (key) were organized into distinct communities through shared CDR3β sequence(s) as in Figure 1C. Thickness of edge represents numbers of shared CDR3β sequence(s) between any two connected nodes. (**F**) Community plot as in (**E**). Color of edge represents shared CDR3β sequence(s) between specificity groups with identical (red) or distinct (blue) specificities defined by tetramer-derived sequences (labeled with distinct colors, **E**). 588 of all (n=634) connections (edges) are labeled in red (92.74%). (**G**) 71 clonally expanded specificity groups as in (**C**). Color of edge represents shared CDR3β sequence(s) between specificity groups with identical (red) or distinct (blue) specificities defined by tetramer-derived sequences (**C**). 92 of all (n=92) connections (edges) are labeled in red (100%). (**H**-**J**) TCR specificity group saturation is dependent of the level of clonal expansion, the absolute numbers of specificity groups, as well as the sequencing depth of the repertoires. (**H**) Bootstrapping for quantification of clonally expanded (right, n=77) and non-expanded (left, n=77) *HLA-A*02:01*-enriched specificity groups with CDR3β sequences from either HLA-A02$^+$ (red) or HLA-A02$^-$ (blue) NSCLC patients. Bootstrapping was done by "sampling with replacement" and the X axis represents the number of patients randomly sampled (Sampled patient #, Methods) and the Y axis represents the numbers of specificity groups quantified with a given sampling event. Shades of error bars represent the 3X standard errors derived from 100 sampling events

for a given number of sampled patients. (**I**) Bootstrapping for quantification of *HLA-A*02:01*-enriched specificity groups with varying cutoffs for *HLA-A*02:01* enrichment ($p < 0.05$, n=1267; $p < 0.025$, n=319; $p < 0.01$, n=72). As in (**H**), X axis represents the number of patients randomly sampled (Sampled patient #). Y axis represents the numbers of specificity groups quantified with a given sampling event that are normalized against the number of the total specificity groups used (Specificity fraction). Shades of error bars represent the 3X standard errors derived from 100 sampling events for a given number of sampled patients. (**J**) Bootstrapping for quantification of *HLA-A*02:01*-enriched specificity groups with varying input CDR3β sequencing depth (50, 75, 87.5, or 100% of total input by random down-sampling). As in (**I**), X axis represents the number of patients randomly sampled and Y axis represents the normalized numbers of specificity groups. Shades of error bars represent the 3X standard errors derived from 100 sampling events for a given number of sampled patients.

Figure S2

A

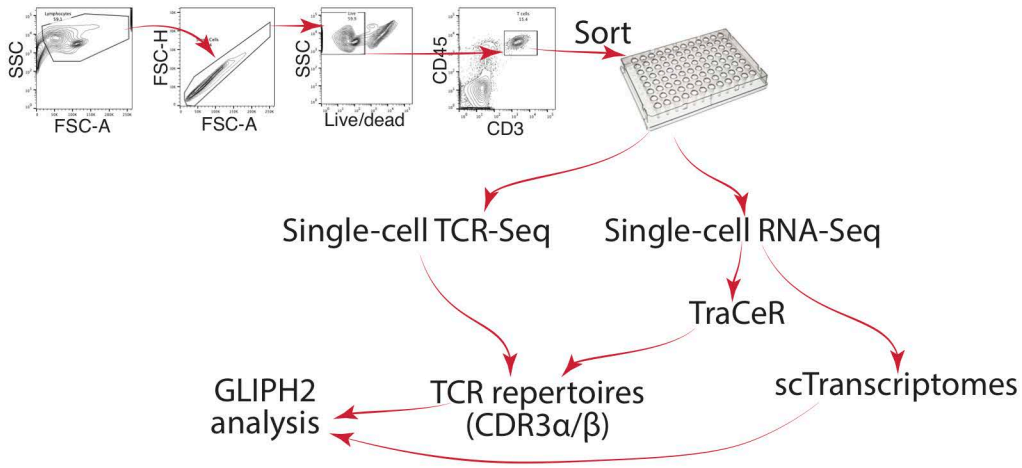

B

Flu-related

Specificity group ID SV%SNQP

TCRβ	Vβ
CASSVaSNQPQHF	TRBV9-1
CASSVdSNQPQHF	TRBV9-1
CASSVeSNQPQHF	TRBV6-8
CASSVfSNQPQHF	TRBV19-1
CASSVgSNQPQHF	TRBV9-1
CASSVkSNQPQHF	TRBV9-1
CASSVlSNQPQHF	TRBV6-8
CASSVnSNQPQHF	TRBV10-2
CASSVsSNQPQHF	TRBV19-1
CASSVtSNQPQHF	TRBV4-2
CASSVySNQPQHF	TRBV19-1

TCR12 clone
α **CATDDSGGFKTIF**
β **CASSVTSNQPQHF**

Specificity group ID SIRS%YE

TCRβ	Vβ
CASSIRStYEQYF	TRBV19-1
CASSIRSgYEQFF	TRBV19-1
CASSIRSgYEQYF	TRBV19-1
CASSIRSdYEQYF	TRBV19-1
CASSIRSeYEQYF	TRBV19-1
CASSIRSaYEQFF	TRBV19-1
CASSIRSaYEQYF	TRBV19-1

TCR13 clone
α **CAGPTGGGSQGNLIF**
β **CASSIRSAYEQYF**

Specificity group ID S%RSTDT

TCRβ	Vβ
CASSkRSTDTQYF	TRBV19-1
CASSdRSTDTQYF	TRBV2-1
CASShRSTDTQYF	TRBV19-1
CASSsRSTDTQYF	TRBV19-1
CASSlRSTDTQYF	TRBV19-1
CASSeRSTDTQYF	TRBV10-2
CASSsRSTDTQYF	TRBV6-8

TCR14 clone
α **CAVTYGGSQGNLIF**
β **CASSSRSTDTQYF**

EBV-related

Specificity group ID RTG%GNT

TCRβ	Vβ
CATRTGgGNTIYF	TRBV6-8
CASRTGpGNTIYF	TRBV9-1
CSARTGtGNTIYF	TRBV29-1
CASRTGdGNTIYF	TRBV9-1
CSARTGvGNTIYF	TRBV20-1
CSVRTGaGNTIYF	TRBV29-1
CAYRTGsGNTIYF	TRBV30-1
CASRTGsGNTIYF	TRBV6-8

TCR15 clone
α **CAEDLNARLMF**
β **CSARTGVGNTIYF**

C

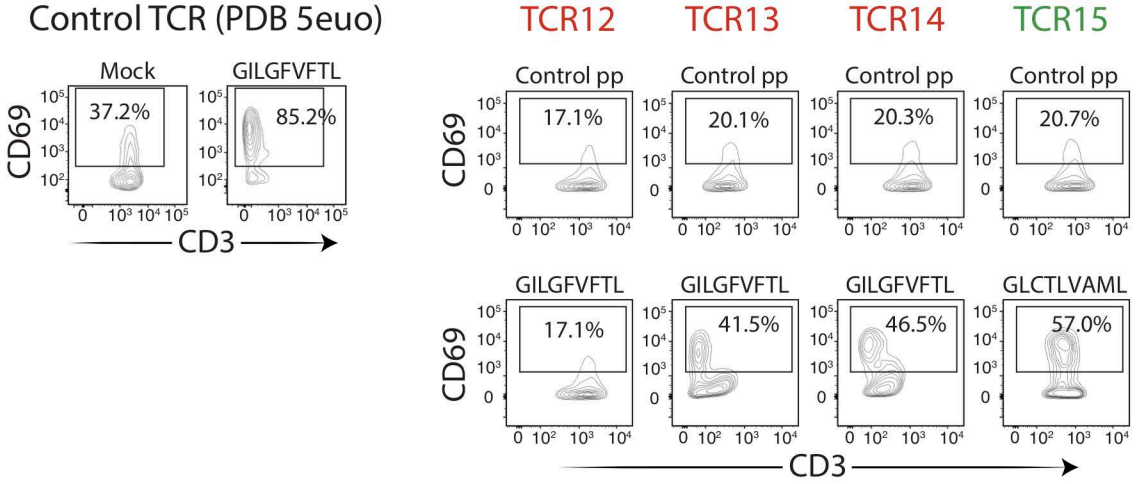

Figure S2, related to Figure 2

(**A**) Schematic of the combined single-cell TCR-Seq and single-cell RNA-Seq (scRNA-seq) procedures. $CD45^{+}CD3^{+}$ T cells were sorted from single-cell suspensions of lung tumor samples from patients with NSCLC at Stanford. Single-cell TCR-Seq was performed using nested multiplexed PCR as previously described [Han *et al*., 2014. Nat. Biotechnol. 32, 684]. scRNA-seq was performed according to previous methods [Picelli *et al*., 2014. Nat. Protoc. 9, 171] with modifications (STAR Methods). TCR repertoires were integrated from the single-cell TCR-Seq pipeline and from the scRNA-seq data with reconstruction using the TraCeR algorithm [Stubbington *et al*., 2016. Nat. Methods 13, 329] for GLIPH2 analysis. scTranscriptomes, single-cell transcriptomes derived from scRNA-seq. (**B**) GLIPH2 inferred clone TCR12, TCR13, and TCR14 to recognize Influenza virus M1 (FluM1) 9mer peptide "GILGFVFTL" in the context of HLA-A*02; clone TCR15 is inferred to recognize EBV BMLF1 9mer peptide "GLCTLVAML" in the context of HLA-A*02. Tables show subsets of CDRβ members for each specificity group. The selected T cell clones with paired CDR3α/β sequences are highlighted in bold in the tables and the CDR3 sequences of both TCRα/β chains are shown at the bottom. All four clones were found in tumors from 2 different NSCLC patients from the Stanford cohort. (**C**) Right, the TCR α/β sequences of the four chosen T cell clonotypes in (**B**) were ectopically expressed in TCR-deficient Jurkat-76 cells and stimulated with T2 ($HLA\text{-}A02^{+}$) cells pulsed with indicated peptides (right, above FACS plots). CD69 expression quantified by FACS is shown. Left, Jurkat cells expressing the control TCRα/β chains (PDB 5euo) previously reported to recognize FluM1 in the context of HLA-A*02 and stimulated with or without (Mock) the 9mer peptide "GILGFVFTL" are shown. Control peptide (pp), $CMV/pp65_{495\text{-}503}$.

Figure S3

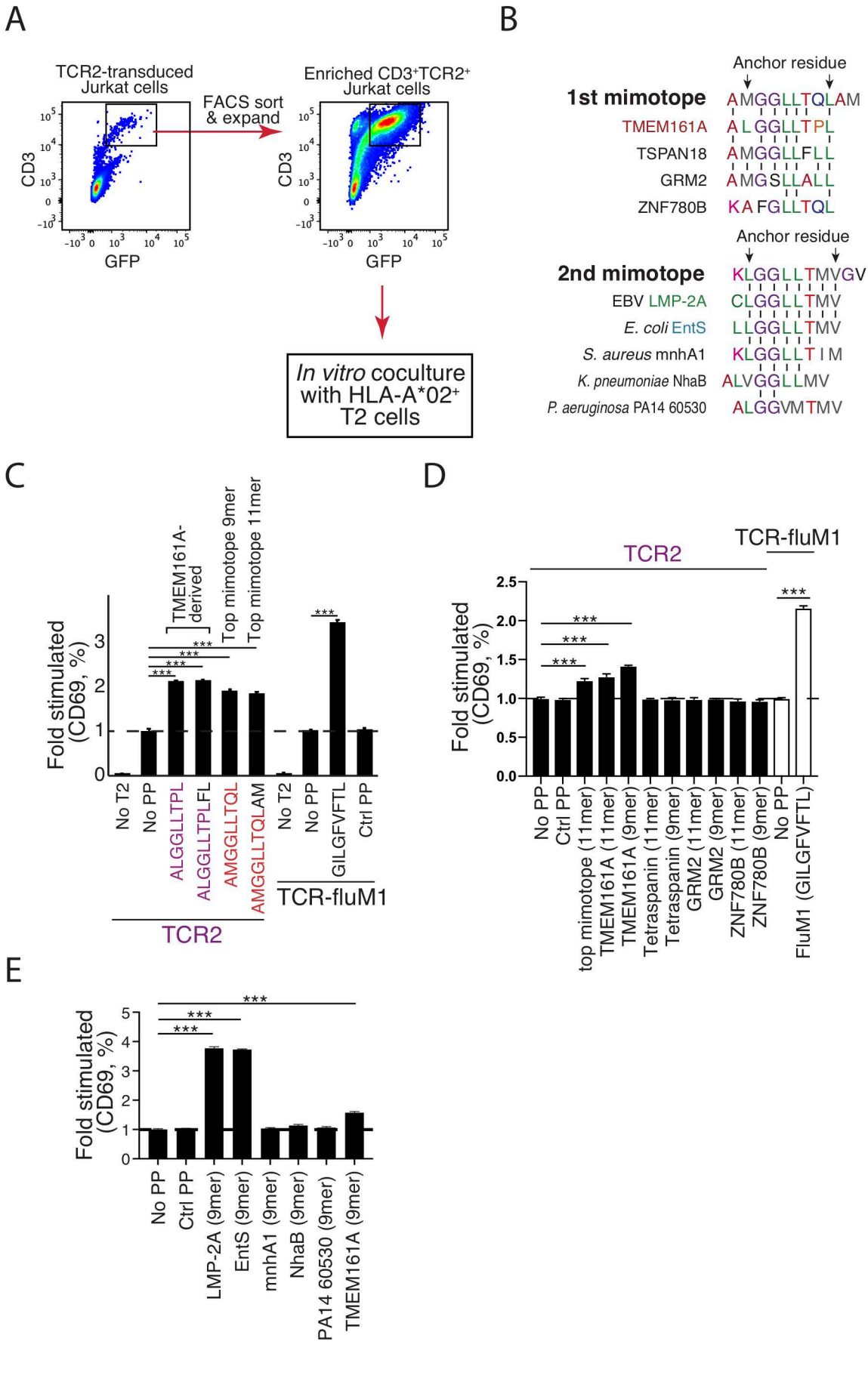
A
TCR2-transduced Jurkat cells
FACS sort & expand
Enriched CD3+TCR2+ Jurkat cells
CD3
GFP
In vitro coculture with HLA-A*02+ T2 cells
B
Anchor residue
1st mimotope
AMGGLLTQLAM
TMEM161A
ALGGLLTPL
TSPAN18
AMGGLLFLL
GRM2
AMGSLLALL
ZNF780B
KAFGLLTQL
Anchor residue
2nd mimotope
KLGGLLTMVGV
EBV LMP-2A
CLGGLLTMV
E. coli EntS
LLGGLLTMV
S. aureus mnhA1
KLGGLLTIM
K. pneumoniae NhaB
ALVGGLLMV
P. aeruginosa PA14 60530
ALGGVMTMV
C
Fold stimulated (CD69, %)
TMEM161A-derived
Top mimotope 9mer
Top mimotope 11mer
No T2
No PP
ALGGLLTPL
ALGGLLTPLFL
AMGGLLTQL
AMGGLLTQLAM
No T2
No PP
GILGFVFTL
Ctrl PP
TCR2
TCR-fluM1
D
TCR2
TCR-fluM1
Fold stimulated (CD69, %)
No PP
Ctrl PP
top mimotope (11mer)
TMEM161A (11mer)
TMEM161A (9mer)
Tetraspanin (11mer)
Tetraspanin (9mer)
GRM2 (11mer)
GRM2 (9mer)
ZNF780B (11mer)
ZNF780B (9mer)
No PP
FluM1 (GILGFVFTL)
E
Fold stimulated (CD69, %)
No PP
Ctrl PP
LMP-2A (9mer)
EntS (9mer)
mnhA1 (9mer)
NhaB (9mer)
PA14 60530 (9mer)
TMEM161A (9mer)

Figure S3, related to Figure 3

(**A**) TCR-deficient Jurkat cells were transduced with lentivirus carrying a composite coding region of TCR2α chain, 2A peptide sequence (2Ap), TCR2β chain, 2Ap, and GFP (Jurkat-TCR2). Transduced cells were subsequently sorted by FACS for the GFP^+CD3^+ population (left) and allowed to expand (top right) and used in *in vitro* stimulation experiments (bottom right). Similar strategies were used to make other stable TCR-Jurkat clones throughout the paper. (**B**) Protein database search showed partial matches of the top 2 mimotopes with candidate coding sequences from various species. All matches were 9mers and predicted to bind HLA-A*02 with high affinities by netMHCpan 4.0. (**C**) Jurkat-TCR2 was stimulated with T2 ($HLA\text{-}A2^+$) cells pulsed with indicated peptides, including the top mimetope from the yeast screen (11mer, AMGGLLTQLAM), the 9mer from the top mimetope predicted to bind HLA-A*02 with high affinity (AMGGLLTQL), and both 9mer/11mer peptides from the TMEM161A coding region (ALGGLLTPL and ALGGLLTPLFL, respectively) with sequence homology to the top mimetope. CD69 upregulation was quantified by FACS. Jurkat cells expressing the control TCRα/β chains (TCR-fluM1, PDB 5euo) and stimulated with the cognate 9mer "GILGFVFTL", the control peptide (Ctrl PP, $CMV/pp65_{495\text{-}503}$), no peptide (No PP), or no co-cultured T2 cells are included as controls. ***, $p < 0.001$ by t test. (**D**,**E**) The endogenous peptides derived from human TMEM161A, LMP-2A of EBV, and EntS of *E. coli* were recognized by TCR2. Jurkat-TCR2 cells were cocultured with $HLA\text{-}A02^+$ T2 cells and pulsed with indicated peptides: Ctrl PP (control peptide), $Flu/M1_{58\text{-}66}$ GILGFVFTL; top mimetope 11mer, AMGGLLTQLAM; TMEM161A 11mer, ALGGLLTPLFL; TMEM161A 9mer, ALGGLLTPL; Tetraspanin 11mer, AMGGLLFLLGF; Tetraspanin 9mer, AMGGLLFLL; GRM2 (Glutamate receptor) 11mer, AMGSLLALLAL; GRM2 9mer, AMGSLLALL; ZNF780B (Zinc finger protein 780B isoform X1) 11mer, KAFGLLTQLAQ; ZNF780B 9mer, KAFGLLTQL in (**D**) and Ctrl PP (control peptide), $Flu/M1_{58\text{-}66}$ GILGFVFTL; LMP-2A 9mer, CLGGLLTMV; EntS 9mer, LLGGLLTMV; mnhA1 9mer, KLGGLLTIM; NhaB 9mer, ALVGGLLMV; PA14 60530 9mer, ALGGVMTMV; TMEM161A 9mer, ALGGLLTPL in (**E**). Jurkat cells expressing the control TCR (TCR-fluM1, PDB 5euo) are stimulated with the cognate 9mer "GILGFVFTL" for comparison.

Figure S4

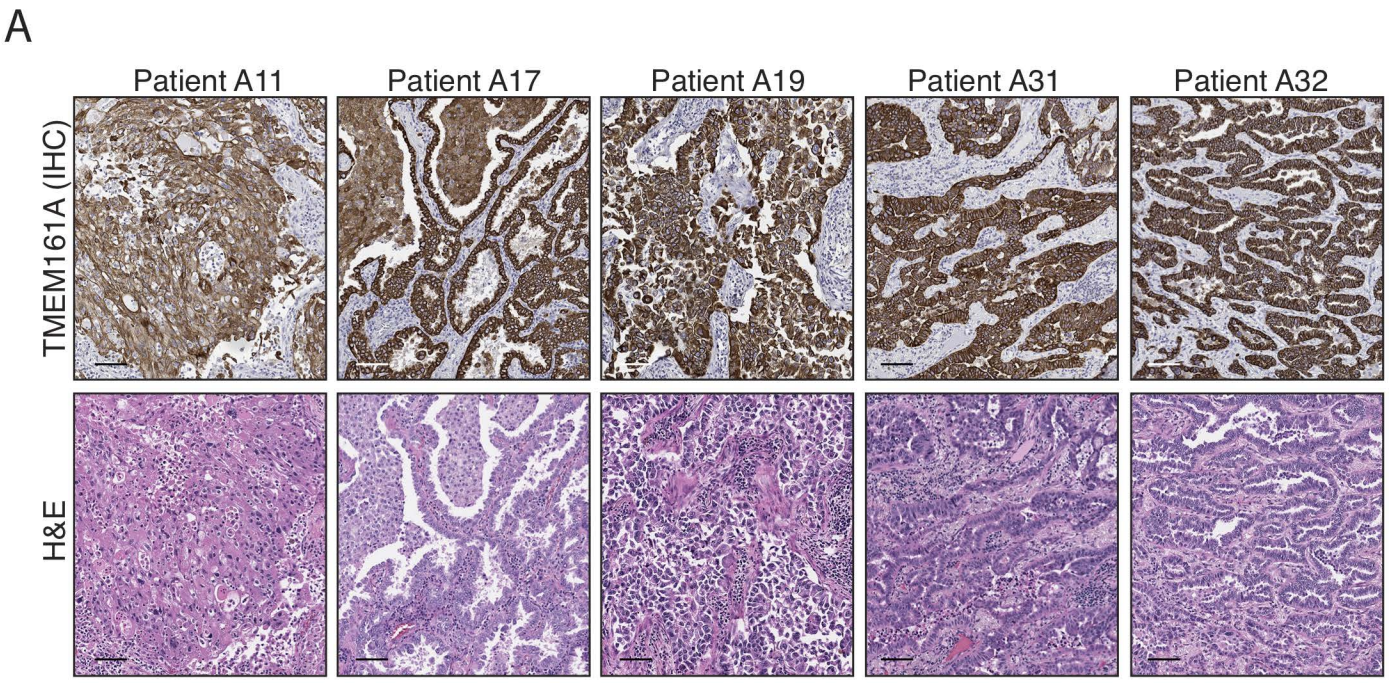

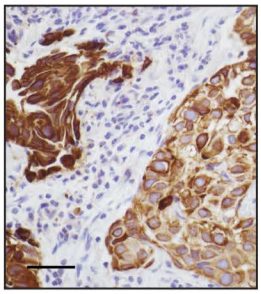

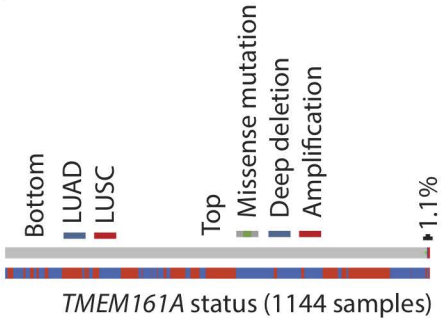

Mutation type	Count
Missense mutation	4
Deep deletion	2
Amplification	6
No alterations	1132

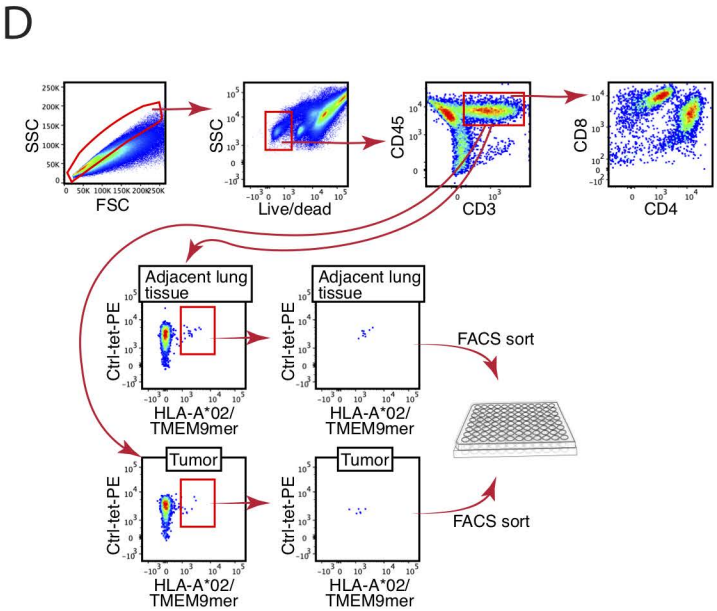

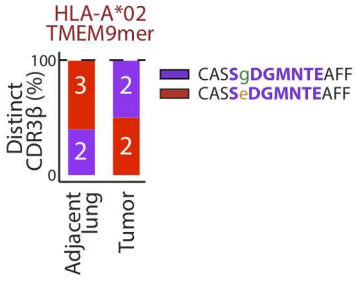

F

S%DGMNTE	LUSC	LUAD
+	21	10
—	16	31

$p = 5.3 \times 10^{-3}$

Figure S4, related to Figure 4

(**A**) TMEM161A is broadly expressed on human NSCLC tumors. Representative images of TMEM161A immunohistochemistry on tumor (top) and hematoxylin & eosin (H&E) staining from adjacent sections (bottom) from Stanford patients A11, A17, A19, A31, and A32. Scale bar, 100 μm. (**B**) Strong and dim TMEM161A staining on a section from A6 patient tumor. Scale bar, 40 μm. (**C**) TMEM161A is a non-mutated tumor antigen. Left, percentages of all types of genetic alterations within the TMEM161A locus defined with whole-genome sequencing from the Cancer Genome Atlas (TCGA) project (pan-lung cancer cases, n=1144) are shown. Right, number of cases with indicated genomic alterations. (**D,E**) TMEM9mer/A02 tetramer^{+} sorted T cells from tumor and the adjacent lung tissue carry the "S%DGMNTE" motif, as predicted by GLIPH2. (**D**) Sorting HLA-A*02/TMEM9mer^{+}CD8^{+} T cells from the resected tumor and the adjacent lung tissue of NSCLC patient A6 through FACS. Single cell suspensions were prepared and stained with anti-CD4, CD8, CD3, and CD45 antibodies, live/dead marker AquaZombie, PE-conjugated tetramer HLA-A*02/viral peptides (CMV-pp65$_{495\text{-}503}$ and EBV-BMLF1$_{280\text{-}288}$), and APC-conjugated tetramer HLA-A*02/TMEM9mer. Specific T cells were sorted onto 96-well plates based on the following criteria: non-doublets, live cells, CD3^{+}CD45^{+}, HLA-A*02/viral peptides^{-}, and HLA-A*02/TMEM9mer^{+}. (**E**) Percentages (%) of distinct CDR3β sequences of tetramer-sorted CD8^{+} T cells as in (**D**) from the adjacent lung tissue and tumor are shown. Numbers in bars represent the counts of sorted cells. (**F**) Numbers of A02^{+} squamous cell lung carcinoma (LUSC) or lung adenocarcinoma (LUAD) patients from the MDACC cohort with or without detected T cells carrying the "S%DGMNTE" CDR3β motif. *p* value = 5.3 x 10^{-3} by Fisher's Exact test.

Figure S5

A

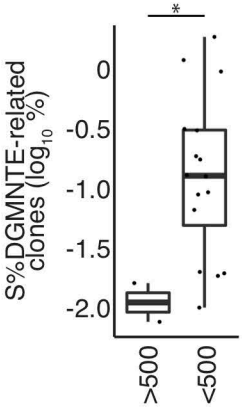

B

	With S%DGMNTE motif	Without S%DGMNTE motif	Fisher's exact test
# Patients	32	47	
Gender			
M	16/32 (50%)	29/47 (62%)	ns
F	16/32 (50%)	18/47 (38%)	ns
Race			
Caucasian	31/32 (97%)	43/47 (91%)	ns
Other	1/32 (3%)	4/47 (9%)	ns
Histology			
Adenocarcinoma	10/32 (31%)	31/47 (66%)	p < 0.01
Squamous cell carcinoma	21/32 (65%)	16/47 (34%)	p < 0.01
Smoking status			
Current smoker	16/32 (50%)	21/47 (45%)	ns
Former smoker	16/32 (50%)	21/47 (45%)	ns
Never smoker	0/32 (0%)	5/47 (11%)	ns
Stage			
I	13/32 (41%)	23/47 (49%)	ns
II	16/32 (50%)	18/47 (38%)	ns
III	3/32 (9%)	6/47 (12%)	ns
Primary tumor size (cm)	4.6	3.8	ns
Adjuvant chemotherapy	12/30 (40%)	14/46 (30%)	ns
Multifocal disease	5/32 (16%)	5/47 (11%)	ns

C

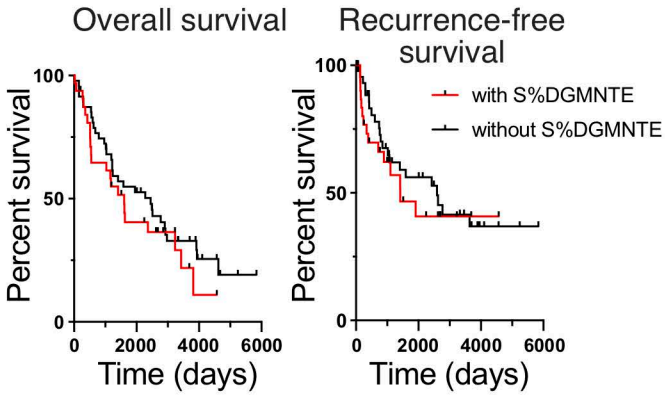

D

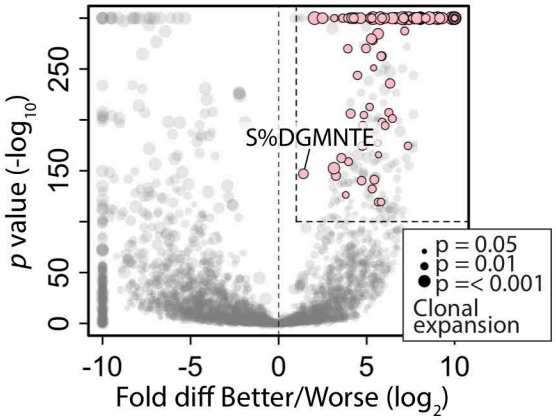

E

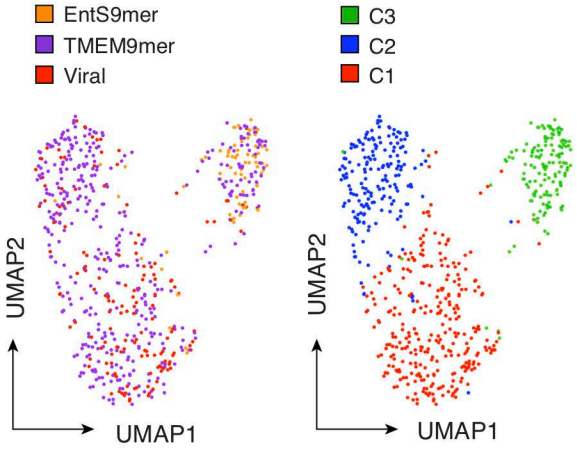

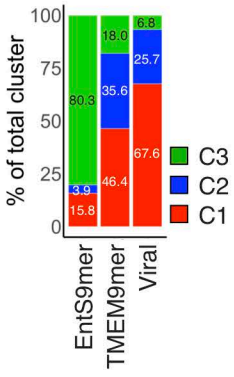

F

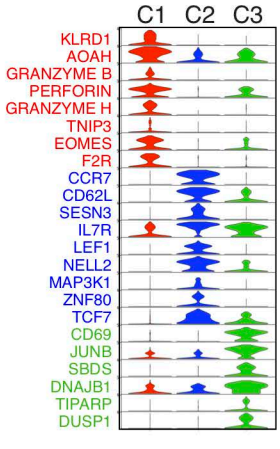

Figure S5, related to Figure 5

(**A**) Total percentage (log_{10}) of T cells carrying the "S%DGMNTE" CDR3β motif for $A02^+$ patients from the MDACC cohorts stratified as having more than 500 (>500) or less than 500 (<500) total mutation counts (n = 34). (**B**) Break down of the clinical data of the MDACC NSCLC patient cohort stratified by detection of CDR3β sequences carrying the "S%DGMNTE" sequence motif. (**C**) There are no differences in overall survival (left) or recurrence-free survival (right) among patients with tumor-infiltrating T cell CDR3β containing the "S%DGMNTE" sequence motif (n = 32) vs patients without tumor-infiltrating T cell CDR3β containing the same motif (n = 49). (**D**) Volcano plot showing the probabilities of clonal biases for the 4,226 clonally expanded specificity groups between the tumors from patients with (worse, n = 88) or without recurrence (better, n = 90) by Poisson test. Tumor-enriched specificity groups that show a significant clonal bias in patients without recurrence are highlighted in pink (n = 146). Specificity group S%DGMNTE is highlighted. (**E**,**F**) A subset of TMEM161A-specific T cells found in healthy donors' peripheral blood reveal effector phenotype. (**E**) Dimension reduction by Uniform Manifold Approximation and Projection (UMAP) of the scRNA-Seq results from the sorted $CD45^+CD8^+CD3^+$ T cells from PBMC with indicated HLA-A*02 tetramers (left) as in Fig 5A identified 3 major cell states (right, # indicates percentage of each cell state). Viral, CD8 T cells sorted with HLA-A*02 tetramers loaded with Flu, EBV, or CMV peptides (Flu-$M1_{58\text{-}66}$, CMV-$pp65_{495\text{-}503}$,and EBV-$BMLF1_{280\text{-}288}$). (**F**) Stacked violin plot showing the differential genes expressed by the identified cell states as in (**E**).

Figure S6

A

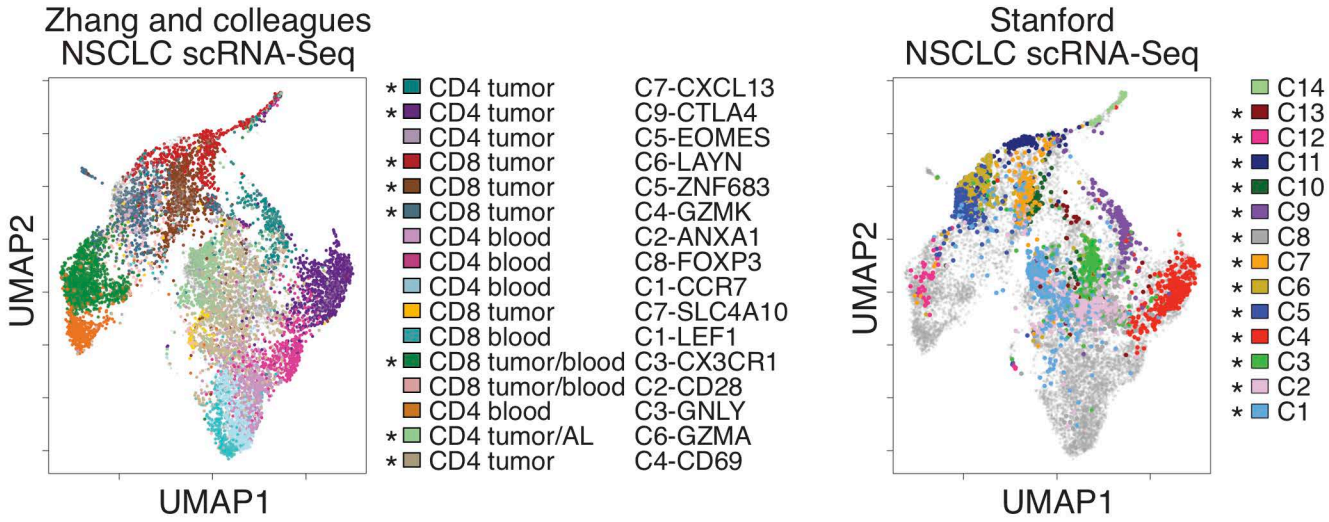

B

Cluster ID (Stanford)	Lineage (Stanford)	Cluster ID (Guo)	Lineage (Guo)	Location (Guo)
C1	CD4	C6-GZMA	CD4	T and AL
C2	CD4	C4-CD69	CD4	T
C3	CD4	C4-CD69	CD4	T
C4	CD4	C9-CTLA4	CD4	T
C5	CD8	C4-GZMK	CD8	T
C6	CD8	C4-GZMK	CD8	T
C7	CD8	C5-ZNF683	CD8	T
C8	CD4	C4-CD69	CD4	T
C9	CD4	C7-CXCL13	CD4	T
C10	CD8	C5-ZNF683	CD8	T
C11	CD8	C6-LAYN	CD8	T
C12	CD8	C3-CX3CR1	CD8	*PB and T
C13	CD4	C4-GZMK/C4-CD69	CD8/CD4	T/T
C14	CD4/CD8	-	-	-

C

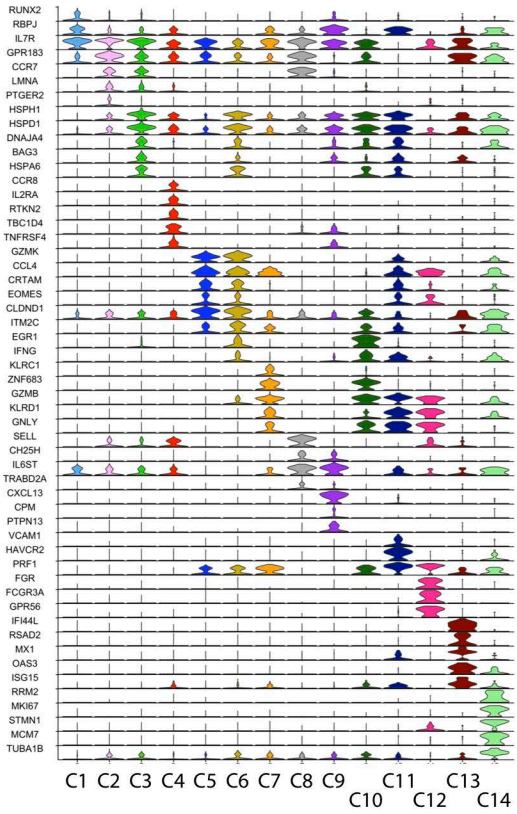

Figure S6, related to Figure 6

(**A**) Dimension reduction by UMAP of the published NSCLC scRNA-Seq results from Zhang and colleagues (Guo *et al*. 2018. Nat. Med. 24, 978). 12,346 sorted T cells from the report by Zhang and colleagues were combined with the 2,950 sorted T cells from the current study (Stanford cohort) for a joint analysis of dimension reduction by UMAP. Cells from Zhang and colleagues are colored according to the identified cell states as reported (left) in comparison with cells from the Stanford cohort colored with the 14 cell states identified in the current study (right). *, cell states identified by Zhang and colleagues (left) that mostly resembled at least one of the cell states identified in the current study (*, right). AL, adjacent lung. (**B**) Cross reference of the 14 cell clusters (C1-C14) identified in the Stanford lung cancer cohort with the clusters reported by Guo *et al*. (Guo *et al*. 2018. Nat. Med. 24, 978). *, CD8 T cells of the C3-CX3CR1 cluster could be found in both the peripheral blood and tumor (Guo *et al*. 2018. Nat. Med. 24, 978). T, tumor; AL, adjacent lung tissue; PB, peripheral blood. (**C**) Selected top differentially expressed genes for each of the identified clusters (n = 14). Expression of indicated genes were shown with the violin plot.

Figure S7

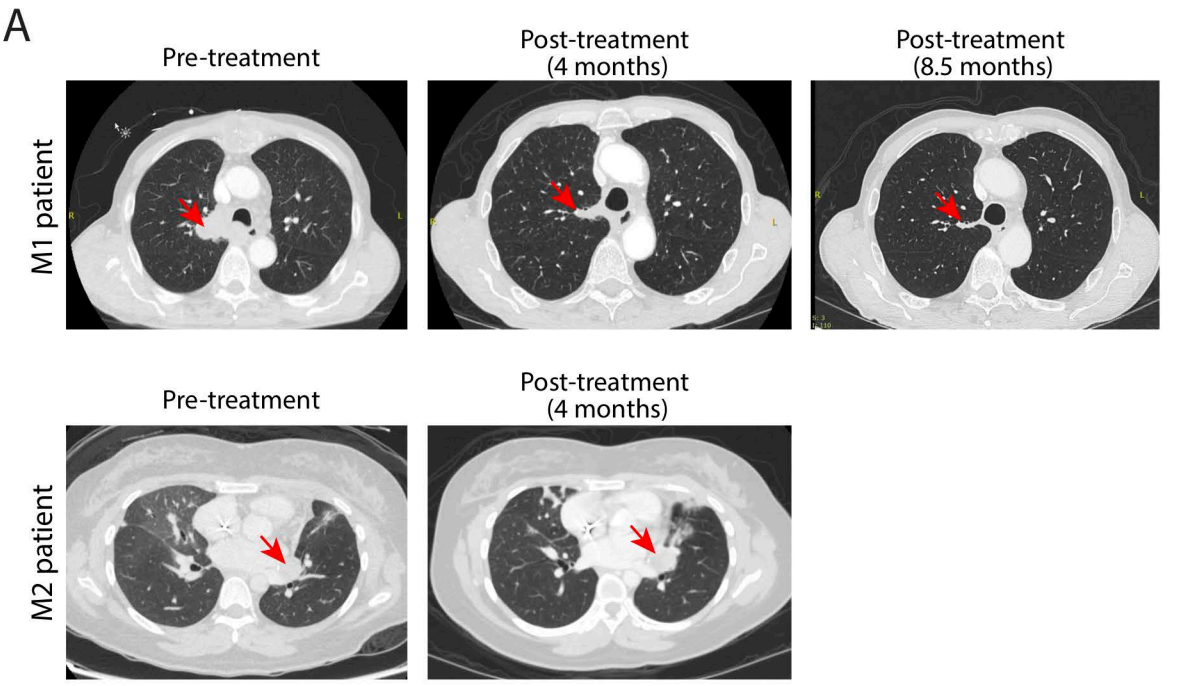
A
Pre-treatment
Post-treatment (4 months)
Post-treatment (8.5 months)
M1 patient
Pre-treatment
Post-treatment (4 months)
M2 patient

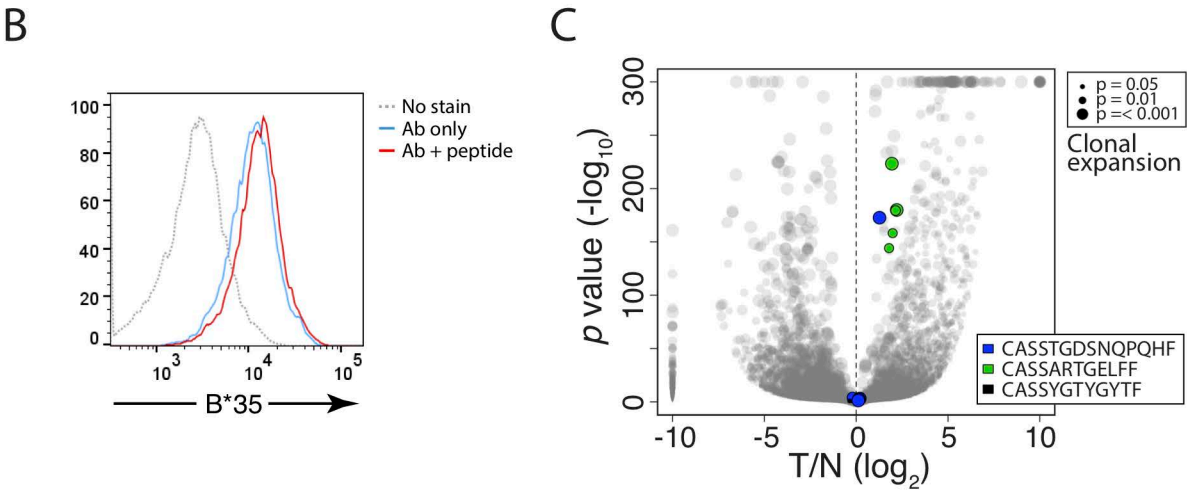
B
No stain
Ab only
Ab + peptide
B*35
C
p value (-log10)
T/N (log2)
p = 0.05
p = 0.01
p =< 0.001
Clonal expansion
CASSTGDSNQPQHF
CASSARTGELFF
CASSYGTYGYTF

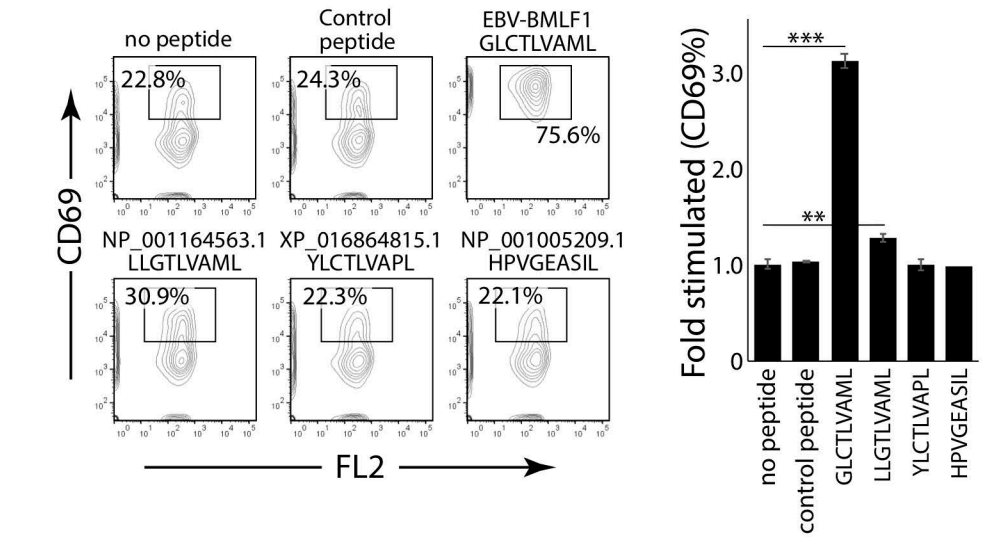
D
no peptide
Control peptide
EBV-BMLF1 GLCTLVAML
22.8%
24.3%
75.6%
NP_001164563.1 LLGTLVAML
XP_016864815.1 YLCTLVAPL
NP_001005209.1 HPVGEASIL
30.9%
22.3%
22.1%
CD69
FL2
Fold stimulated (CD69%)
***
**
no peptide
control peptide
GLCTLVAML
LLGTLVAML
YLCTLVAPL
HPVGEASIL

Figure S7, related to Figure 7

(**A**) CT scan images of pre- and post-treatment from NSCLC patient M1 (top panels) and M2 (bottom panels) treated with anti-PD1 therapy. Tumors are highlighted with red arrowheads. (**B**) T2 (174 x CEM.T2) cells were transduced with lentiviral vector encoding the full-length coding sequence of WT human *HLA-B*35:01*. Cells were selected with puromycin and the surface B*35 expression was quantified by FACS with or without the control peptide "LPFDFTPGY" reported previously (Takamiya *et al.*, 1994. Int Immunol. Vol. 6, 255). (**C**) Volcano plot showing the comparison of the 66,094 shared specificity groups between tumor (T) and the adjacent lung (N) by Poisson test. The y-axis represents the negative $\log_{10}$ converted *p* values of the Poisson tests and the x-axis represents the $\log_2$ converted fold difference between tumor and the adjacent lung (T/N). Dot size represents levels of clonal expansion. Specificity groups annotated with pathogen-related tetramer CDR3β sequences as in Figure 7B (n=11) are highlighted according to the respective CDR3β sequences of the expanded clones (5th column, Figure 7B). (**D**) Left panels, representative FACS plots showing the stimulation of the Jurkat-TCR15 cells with 9mers from the EBV *BMLF1* locus (GLCTLVAML), uniprot NP_001164563.1 (*CLDN2* locus, LLGTLVAML), XP_016864815.1 (*SERINC5* locus, YLCTLVAPL), and NP_001005209.1 (*TMEM198* locus, GLLCGLVAML). Right, results of Jurkat-TCR15 cell stimulation in triplicate. Control peptide: flu M1 "GILGFVFTL". ***, $p < 0.001$; **, $p < 0.01$ by student t test.

Table S1, related to Figure 1.

Patient ID	Lesion type	Gender	Ethnicity	HLA-A	HLA-A	HLA-B	HLA-B	HLA-C	HLA-C
MDA-1150	SCC	F	Caucasian	A*01:01	A*02:01	B*37:01	B*08:01	C*06:02	C*07:01
MDA-1170	SCC	F	Caucasian	A*02:01	A*02:01	B*67:01	B*50:01	C*12:03	C*06:02
MDA-1193	ADC	F	Caucasian	A*26:01	A*24:02	B*07:02	B*07:02	C*05:01	C*07:02
MDA-1206	SCC	M	Caucasian	A*03:01	A*03:01	B*57:01	B*14:02	C*08:01	C*08:02
MDA-1214	SCC	M	Hispanic	A*24:02	A*11:01	B*44:03	B*45:01	C*05:01	C*06:02
MDA-1248	SCC	M	Caucasian	A*31:01	A*02:01	B*35:01	B*07:02	C*07:02	C*04:01
MDA-1264	ADC	M	Caucasian	A*32:01	A*02:01	B*13:02	B*44:02	C*05:01	C*06:02
MDA-1273	SCC	M	Caucasian	A*66:01	A*03:01	B*15:16	B*08:01	C*17:01	C*14:02
MDA-1278	ADC	F	Caucasian	A*02:01	A*02:01	B*18:01	B*44:02	C*07:01	C*12:03
MDA-1283	SCC	M	Caucasian	A*29:02	A*02:51	B*14:02	B*27:05	C*01:02	C*08:02
MDA-1321	SCC	M	Caucasian	A*24:02	A*03:01	B*51:01	B*81:03	C*07:02	C*01:02
MDA-1339	SCC	F	Caucasian	A*03:01	A*01:01	B*42:01	B*07:02	C*07:01	C*07:02
MDA-1346	ADC	F	Caucasian	A*02:60	A*02:03	B*15:01	B*44:09	C*05:01	C*03:03
MDA-1356	ADC	M	Caucasian	A*32:01	A*03:26	B*40:02	B*55:22	C*01:02	C*02:02
MDA-1361	SCC	M	Caucasian	A*25:01	A*02:01	B*40:01	B*44:02	C*03:04	C*05:01
MDA-1366	SCC	M	Caucasian	A*03:26	A*03:04	B*07:02	B*35:01	C*07:02	C*04:01
MDA-1386	SCC	M	Caucasian	A*01:01	A*01:01	B*14:01	B*08:01	C*08:02	C*07:01
MDA-1388	SCC	M	Caucasian	A*29:02	A*03:01	B*35:01	B*44:03	C*16:01	C*04:01
MDA-1392	ADC	F	Caucasian	A*02:01	A*02:01	B*51:01	B*07:02	C*07:02	C*14:02
MDA-1402	SCC	M	African American	A*24:02	A*03:01	B*15:03	B*07:02	C*02:10	C*07:02
MDA-1409	SCC	M	Caucasian	A*24:02	A*01:14	B*08:01	B*55:01	C*01:02	C*07:01
MDA-1413	ADC	M	Caucasian	A*30:04	A*68:01	B*18:01	B*27:05	C*05:01	C*02:02
MDA-1420	SCC	F	Caucasian	A*31:01	A*24:02	B*35:08	B*07:02	C*07:02	C*04:01
MDA-1425	SCC	M	Caucasian	A*25:01	A*25:01	B*08:01	B*18:01	C*12:03	C*07:01
MDA-1429	SCC	M	Caucasian	A*30:04	A*02:01	B*07:02	B*18:01	C*05:01	C*07:02
MDA-1450	ADC	F	Caucasian	A*26:01	A*02:03	B*35:01	B*44:02	C*05:08	C*04:01
MDA-1453	ADC	F	Caucasian	A*02:01	A*03:01	B*07:02	B*44:02	C*05:01	C*07:02
MDA-1455	SCC	M	Caucasian	A*02:01	A*02:01	B*07:02	B*44:09	C*05:01	C*07:02
MDA-1463	SCC	M	Caucasian	A*31:01	A*02:01	B*40:01	B*44:02	C*05:01	C*03:04
MDA-1489	SCC	M	Caucasian	A*31:01	A*01:01	B*08:01	B*18:01	C*05:01	C*07:01
MDA-1514	ADC	F	Caucasian	A*26:01	A*02:01	B*50:01	B*27:05	C*01:02	C*06:02
MDA-1517	SCC	F	Caucasian	A*26:01	A*02:03	B*07:02	B*27:05	C*07:02	C*01:02
MDA-1520	SCC	M	Caucasian	A*29:02	A*29:05	B*51:01	B*51:42	C*15:02	C*05:01
MDA-1530	SCC	M	Caucasian	A*03:01	A*02:01	B*07:02	B*07:02	C*07:02	C*07:02
MDA-1532	SCC	M	Caucasian	A*02:01	A*02:01	B*51:01	B*57:02	C*16:02	C*07:01
MDA-1549	SCC	M	Caucasian	A*11:01	A*24:02	B*15:02	B*15:02	C*08:01	C*08:01
MDA-1550	ADC	F	Caucasian	A*02:02	A*02:01	B*13:02	B*15:01	C*06:02	C*03:03
MDA-1556	SCC	F	Caucasian	A*02:01	A*02:01	B*18:03	B*35:01	C*07:01	C*04:01
MDA-1560	ADC	F	African American	A*03:01	A*03:01	B*07:02	B*57:01	C*06:02	C*07:02
MDA-1570	SCC	M	African American	A*68:02	A*29:02	B*07:02	B*07:02	C*07:02	C*16:01
MDA-1587	SCC	M	Caucasian	A*02:01	A*01:01	B*57:01	B*44:02	C*05:01	C*06:02
MDA-1600	SCC	M	Caucasian	A*11:01	A*02:01	B*35:01	B*44:03	C*02:02	C*04:01
MDA-1612	SCC	F	Caucasian	A*02:266	A*01:01	B*49:01	B*57:01	C*06:02	C*12:03
MDA-1615	SCC	F	African American	A*29:02	A*29:02	B*81:01	B*07:02	C*18:01	C*14:02
MDA-1636	ADC	M	Caucasian	A*32:01	A*11:01	B*15:01	B*14:01	C*08:02	C*03:03
MDA-1649	ADC	M	Caucasian	A*24:02	A*03:01	B*46:01	B*14:02	C*08:02	C*03:13
MDA-1660	SCC	M	Caucasian	A*31:01	A*01:01	B*27:05	B*08:01	C*01:02	C*07:01
MDA-1664	SCC	F	Caucasian	A*26:01	A*11:01	B*38:01	B*52:01	C*12:03	C*12:02
MDA-1708	ADC	M	Caucasian	A*02:05	A*02:05	B*13:02	B*53:01	C*06:02	C*07:18
MDA-1736	ADC	F	Caucasian	A*29:02	A*11:01	B*35:01	B*44:03	C*04:01	C*16:01
MDA-1742	ADC	F	Caucasian	A*01:01	A*24:02	B*15:17	B*35:03	C*07:01	C*12:03
MDA-1743	ADC	M	Caucasian	A*02:68	A*24:02	B*44:02	B*44:03	C*03:03	C*05:01
MDA-1756	SCC	M	Caucasian	A*32:01	A*02:01	B*15:18	B*40:02	C*07:04	C*02:02
MDA-1758	ADC	F	Caucasian	A*02:01	A*01:01	B*51:01	B*08:01	C*07:01	C*15:02
MDA-1769	ADC	M	Caucasian	A*03:01	A*02:01	B*07:02	B*15:01	C*03:03	C*07:02
MDA-1772	SCC	M	Caucasian	A*02:01	A*24:02	B*40:79	B*44:02	C*05:01	C*03:04
MDA-1774	ADC	M	Caucasian	A*02:01	A*02:05	B*49:01	B*15:01	C*03:03	C*07:01
MDA-1775	ADC	F	Caucasian	A*02:01	A*29:02	B*51:01	B*44:03	C*15:02	C*16:01
MDA-1785	SCC	F	Caucasian	A*02:01	A*02:03	B*08:01	B*44:02	C*05:01	C*07:01
MDA-1793	ADC	M	Caucasian	A*24:02	A*24:03	B*46:01	B*51:01	C*14:02	C*01:02
MDA-1818	ADC	F	Caucasian	-	-	B*35:01	B*08:01	C*07:01	C*04:01
MDA-1822	SCC	M	Caucasian	A*02:03	A*02:01	B*41:01	B*44:46	C*07:01	C*05:01
MDA-1823	ADC	M	Caucasian	A*24:03	A*01:01	B*42:01	B*07:02	C*07:01	C*07:02
MDA-1833	ADC	F	Caucasian	A*30:01	A*11:01	B*13:02	B*35:01	C*06:02	C*04:01
MDA-1837	ADC	F	Caucasian	A*03:01	A*03:01	B*35:01	B*07:02	C*07:02	C*04:01
MDA-1845	ADC	F	Caucasian	A*68:02	A*29:02	B*45:01	B*45:01	C*06:02	C*16:01
MDA-1848	ADC	M	Caucasian	A*68:01	A*68:01	B*37:01	B*40:01	C*06:02	C*03:04
MDA-1853	ADC	M	Caucasian	A*03:01	A*03:01	B*07:02	B*07:02	C*07:02	C*07:02
MDA-1872	ADC	M	Caucasian	A*68:01	A*74:01	B*53:01	B*07:02	C*15:05	C*04:01
MDA-1875	ADC	F	Caucasian	A*01:01	A*24:02	B*08:01	B*39:06	C*07:02	C*07:01
MDA-1893	SCC	M	Caucasian	A*02:01	A*02:01	B*57:01	B*35:02	C*04:01	C*06:02
MDA-1896	SCC	M	Caucasian	A*03:26	A*02:01	B*14:02	B*35:03	C*04:01	C*08:02
MDA-1904	ADC	M	Caucasian	A*03:01	A*23:01	B*14:02	B*49:01	C*08:02	C*07:01
MDA-1905	ADC	M	Caucasian	A*02:01	A*02:06	B*07:02	B*07:02	C*03:05	C*07:02
MDA-1906	ADC	M	Caucasian	A*23:01	A*01:01	B*08:01	B*49:01	C*07:01	C*07:01
MDA-1908	SCC	F	Caucasian	A*02:68	A*23:01	B*35:01	B*44:03	C*04:01	C*04:01
MDA-1913	SCC	M	Caucasian	A*02:01	A*29:02	B*44:03	B*18:01	C*07:01	C*16:01
MDA-1914	ADC	M	Caucasian	A*03:01	A*03:01	B*07:02	B*18:01	C*07:02	C*12:03
MDA-1928	SCC	F	Caucasian	A*68:02	A*68:02	B*44:03	B*08:01	C*07:01	C*16:01
MDA-1930	SCC	M	Caucasian	A*32:01	A*32:01	B*44:02	B*41:01	C*17:01	C*05:01
MDA-1937	ADC	M	Caucasian	A*32:01	A*32:01	B*14:02	B*46:01	C*03:03	C*08:02
MDA-1950	SCC	M	Caucasian	A*02:07	A*24:02	B*44:09	B*44:02	C*07:04	C*17:03
MDA-1960	ADC	M	Caucasian	A*31:01	A*29:02	B*08:01	B*07:02	C*07:01	C*07:74
MDA-1971	ADC	M	African American	A*02:01	A*11:01	B*35:01	B*51:01	C*15:02	C*04:01
MDA-1991	SCC	F	Caucasian	A*01:01	A*01:01	B*07:02	B*14:08	C*07:02	C*08:02
MDA-2004	ADC	M	Caucasian	A*03:01	A*03:01	B*39:06	B*35:01	C*07:02	C*04:01
MDA-2016	ADC	F	Caucasian	A*02:01	A*31:01	B*35:03	B*07:02	C*04:01	C*07:02
MDA-2017	ADC	F	Caucasian	A*01:01	A*36:01	B*53:01	B*07:02	C*07:02	C*04:01
MDA-2021	ADC	M	Hispanic	A*34:08	A*33:03	B*35:01	B*35:01	C*06:02	C*16:01
MDA-2022	ADC	M	Caucasian	A*03:01	A*03:01	B*55:02	B*46:01	C*03:03	C*03:04
MDA-2025	ADC	M	Caucasian	A*33:03	A*30:01	B*53:01	B*42:01	C*17:01	C*04:01
MDA-2028	ADC	F	Caucasian	A*11:01	A*11:01	B*15:18	B*44:02	C*05:01	C*08:01
MDA-2031	SCC	M	African American	A*02:01	A*03:01	B*35:01	B*35:01	C*06:02	C*16:01
MDA-2034	SCC	M	Caucasian	A*03:56	A*03:01	B*07:02	B*07:02	C*06:02	C*07:02
MDA-2037	ADC	F	Caucasian	A*32:01	A*24:02	B*49:01	B*35:01	C*07:01	C*04:01
MDA-2040	SCC	M	Caucasian	A*24:02	A*24:02	B*41:01	B*07:02	C*07:01	C*07:02
MDA-2046	ADC	M	Caucasian	A*03:01	A*02:01	B*40:01	B*44:02	C*05:01	C*07:02
MDA-2052	ADC	M	Caucasian	A*02:01	A*68:01	B*38:01	B*15:01	C*12:03	C*04:01

MDA-2054	ADC	F	African American	A*23:01	A*11:01	B*14:02	B*35:01	C*08:02	C*04:01
MDA-2057	SCC	M	Caucasian	A*31:01	A*36:01	B*08:12	B*40:01	C*03:04	C*07:01
MDA-2060	ADC	M	Caucasian	A*01:01	A*01:01	B*08:01	B*08:01	C*06:02	C*07:01
MDA-2061	SCC	F	Caucasian	A*68:01	A*68:01	B*51:01	B*08:01	C*01:02	C*07:01
MDA-2068	SCC	F	Caucasian	A*26:01	A*02:60	B*18:01	B*07:02	C*01:02	C*07:02
MDA-2070	ADC	M	Caucasian	A*03:56	A*03:01	B*51:01	B*35:01	C*04:01	C*15:02
MDA-2080	ADC	F	Caucasian	A*02:01	A*01:01	B*08:01	B*18:01	C*07:01	C*07:01
MDA-2082	ADC	M	Caucasian	A*02:01	A*01:01	B*07:02	B*15:01	C*03:04	C*07:02
MDA-2088	SCC	M	Caucasian	A*11:01	A*02:01	B*55:02	B*55:01	C*05:01	C*03:03
MDA-2090	SCC	M	Caucasian	A*01:01	A*03:56	B*07:02	B*15:17	C*07:01	C*07:01
MDA-2093	ADC	M	African American	A*11:01	A*02:01	B*15:01	B*35:01	C*03:03	C*04:01
MDA-2095	ADC	F	African American	A*02:05	A*03:01	B*50:01	B*07:02	C*06:02	C*07:02
MDA-2097	ADC	M	Caucasian	A*02:05	A*02:51	B*35:02	B*35:01	C*04:01	C*07:18
MDA-2108	SCC	M	Caucasian	A*02:05	A*30:01	B*18:01	B*57:01	C*12:03	C*06:02
MDA-2115	ADC	M	African American	A*03:04	A*03:63	B*51:02	B*51:01	C*15:02	C*03:04
MDA-2118	ADC	F	Asian or Pacific Islander	A*24:02	A*01:01	B*08:01	B*15:01	C*01:02	C*07:01
MDA-2121	SCC	F	Caucasian	A*03:01	A*23:01	B*35:01	B*35:01	C*04:01	C*04:01
MDA-2122	SCC	M	Caucasian	A*31:01	A*31:01	B*27:05	B*40:01	C*03:04	C*02:02
MDA-2139	SCC	M	Caucasian	A*02:01	A*03:26	B*27:02	B*07:02	C*07:02	C*02:02
MDA-2140	SCC	M	Caucasian	A*25:01	A*01:01	B*18:01	B*18:13	C*12:03	C*12:03
MDA-2150	ADC	F	Caucasian	A*03:01	A*03:01	B*27:05	B*07:02	C*07:02	C*01:02
MDA-2152	SCC	M	Caucasian	A*68:01	A*68:01	B*35:01	B*44:02	C*02:02	C*04:01
MDA-2155	SCC	M	Caucasian	A*02:01	A*02:01	B*08:01	B*14:02	C*08:02	C*07:01
MDA-2161	SCC	M	Caucasian	A*25:01	A*02:01	B*18:01	B*44:02	C*05:01	C*12:03
MDA-2175	ADC	M	Caucasian	A*02:01	A*03:01	B*07:02	B*15:01	C*03:04	C*07:02
MDA-2176	ADC	M	Caucasian	A*02:01	A*03:01	B*07:02	B*18:01	C*07:02	C*12:13
MDA-2195	SCC	F	Caucasian	A*33:01	A*03:01	B*14:02	B*08:01	C*08:02	C*07:01
MDA-2214	ADC	F	Caucasian	A*26:01	A*26:01	B*38:01	B*57:01	C*06:02	C*12:03
MDA-2221	ADC	M	Caucasian	A*24:02	A*02:01	B*08:01	B*14:02	C*08:02	C*07:01
MDA-2226	SCC	M	Caucasian	A*31:01	A*02:01	B*35:03	B*35:03	C*04:01	C*04:01
MDA-2230	ADC	M	Caucasian	A*30:02	A*03:01	B*53:01	B*07:02	C*07:19	C*07:01
MDA-2237	ADC	F	Caucasian	A*11:05	A*33:01	B*14:02	B*14:02	C*08:02	C*08:02
MDA-2240	ADC	F	Caucasian	A*26:01	A*29:02	B*27:05	B*44:03	C*01:02	C*16:01
MDA-2243	ADC	M	African American	A*03:01	A*24:02	B*27:05	B*07:02	C*07:02	C*01:02
MDA-2244	ADC	M	Caucasian	A*02:01	A*03:01	B*15:01	B*07:02	C*07:02	C*07:39
MDA-2254	ADC	M	Caucasian	A*26:01	A*11:01	B*51:01	B*15:01	C*15:02	C*04:01
MDA-2262	SCC	M	Caucasian	A*03:01	A*03:01	B*08:01	B*07:02	C*07:02	C*07:01
MDA-2264	SCC	F	Caucasian	A*02:03	A*02:03	B*07:02	B*07:02	C*06:02	C*07:02
MDA-2265	SCC	F	Caucasian	A*03:01	A*03:01	B*07:02	B*18:01	C*05:01	C*07:02
MDA-2271	ADC	F	Caucasian	A*11:01	A*11:01	B*08:01	B*44:02	C*05:01	C*07:01
MDA-2276	ADC	F	Caucasian	A*01:01	A*02:01	B*44:02	B*44:02	C*05:01	C*05:01
MDA-2286	ADC	M	Caucasian	A*24:02	A*02:03	B*40:01	B*51:01	C*03:04	C*01:02
MDA-2292	ADC	M	Caucasian	A*32:01	A*03:01	B*07:02	B*55:01	C*03:03	C*03:03
MDA-2294	ADC	F	Caucasian	A*03:01	A*03:01	B*51:01	B*08:01	C*01:02	C*07:01
MDA-2300	SCC	M	Caucasian	A*24:02	A*24:03	B*08:01	B*08:01	C*07:01	C*07:01
MDA-2307	ADC	M	Caucasian	A*02:01	A*01:01	B*15:01	B*51:01	C*16:02	C*03:04
MDA-2315	ADC	F	Caucasian	A*02:01	A*11:01	B*35:01	B*44:02	C*05:01	C*04:01
MDA-2316	ADC	M	African American	A*03:01	A*03:01	B*08:01	B*35:01	C*07:01	C*04:01
MDA-2318	ADC	F	Caucasian	A*30:26	A*03:01	B*39:01	B*13:02	C*06:02	C*07:02
MDA-2320	ADC	F	Caucasian	A*02:01	A*02:01	B*15:01	B*44:09	C*03:03	C*05:01
MDA-2325	SCC	F	Caucasian	A*26:01	A*24:10	B*18:01	B*13:02	C*06:02	C*07:01
MDA-2333	ADC	M	Caucasian	A*32:01	A*24:02	B*07:02	B*07:02	C*07:02	C*02:02
MDA-2335	ADC	F	Caucasian	A*25:01	A*25:01	B*08:01	B*57:01	C*06:02	C*07:01
MDA-2337	ADC	F	Caucasian	A*24:02	A*02:01	B*15:01	B*15:01	C*03:03	C*03:04
MDA-2343	ADC	M	Caucasian	A*68:02	A*30:02	B*15:10	B*35:01	C*06:02	C*03:02
MDA-2344	SCC	F	Caucasian	A*11:01	A*02:03	B*08:01	B*18:01	C*07:01	C*07:01
MDA-2345	ADC	M	Caucasian	A*01:01	A*01:01	B*08:01	B*08:01	C*07:01	C*07:01
MDA-2348	ADC	F	Caucasian	A*02:01	A*02:01	B*07:02	B*07:02	C*05:01	C*07:02
MDA-2352	ADC	F	Caucasian	A*03:01	A*03:01	B*51:01	B*07:02	C*07:02	C*14:02
MDA-3203	ADC	M	Caucasian	A*02:01	A*11:01	B*35:01	B*07:02	C*04:01	C*07:02
MDA-3212	ADC	F	Caucasian	A*30:01	A*02:01	B*13:02	B*15:01	C*03:61	C*06:02
MDA-3214	ADC	F	Caucasian	A*02:01	A*02:89	B*50:01	B*38:01	C*04:01	C*12:03
MDA-3234	SCC	F	Caucasian	A*03:01	A*02:01	B*51:01	B*35:01	C*02:02	C*04:01
MDA-3237	SCC	F	Caucasian	A*24:02	A*24:02	B*15:07	B*40:01	C*03:03	C*03:04
MDA-3238	ADC	M	African American	A*33:03	A*30:02	B*53:01	B*15:10	C*03:04	C*04:01
MDA-3242	ADC	M	Caucasian	A*25:01	A*25:01	B*15:17	B*18:01	C*07:01	C*12:03
MDA-3253	SCC	F	Caucasian	A*03:01	A*02:01	B*07:02	B*07:02	C*07:02	C*07:02
MDA-3259	ADC	F	Caucasian	A*01:01	A*01:01	B*08:01	B*07:02	C*07:01	C*07:01
MDA-3260	ADC	M	Caucasian	A*29:02	A*29:02	B*44:03	B*57:01	C*16:04	C*06:02
MDA-3273	ADC	M	Asian or Pacific Islander	A*24:02	A*02:01	B*40:06	B*40:01	C*15:02	C*08:01
MDA-3290	SCC	F	Caucasian	A*02:251	A*24:02	B*07:02	B*27:05	C*01:02	C*07:02
MDA-4309	ADC	F	Caucasian	A*02:01	A*02:01	B*27:07	B*08:01	C*01:02	C*07:01
MDA-4347	ADC	F	Caucasian	A*03:01	A*03:02	B*08:01	B*15:01	C*03:04	C*07:39
MDA-4361	ADC	M	Hispanic	A*68:03	A*11:01	B*39:05	B*40:138	C*03:04	C*07:02
MDA-4363	ADCA/SCC	F	Caucasian	A*11:01	A*02:01	B*35:01	B*57:01	C*06:02	C*04:01
MDA-4378	ADC	F	Caucasian	A*29:02	A*11:01	B*51:01	B*44:03	C*15:02	C*16:01
MDA-4382	SCC	M	Hispanic	A*31:01	A*11:01	B*52:01	B*39:06	C*07:02	C*12:02
MDA-4383	ADC	M	Caucasian	A*02:01	A*02:01	B*40:01	B*57:01	C*06:02	C*03:04
MDA-4385	ADC	F	Caucasian	A*26:01	A*26:01	B*37:01	B*08:01	C*06:02	C*07:01
MDA-4386	ADC	M	Caucasian	A*03:01	A*03:01	B*08:01	B*18:01	C*07:01	C*07:01

HLA class I genotypes and clinical attributes for the MDACC NSCLC cohort (Reuben *et al*., 2020 Nat Commun). ADC, adenocarcinoma; SCC, squamous cell carcinoma.

Table S4, related to Figure 2.

Patient ID	scTCR-seq	scRNA-Seq	Histology (tumor)	Histology (adjacent lung tissue)	Exome seq	Age	Gender	HLA-A*02	Smoking (pk yr)	Stage	Histology
A2	yes					65	M	N	50	IB	SCC
A3	yes					71	M	Y	50	IB	SCC
A4	yes		yes			49	M	Y	0	IA	adeno
A5	yes		yes	yes		65	F	N	0	IB	adeno
A6*	yes		yes	yes		73	F	Y	45	IB	SCC
A7			yes	yes		64	M	Y	118	IB	adeno
A8			yes	yes		71	F	Y	60	IB	adeno
A9			yes			77	M	N	45	IB	adeno
A10			yes	yes		82	F	N	0	IIA	adeno
A11	yes	yes	yes	yes	yes	76	F	Y	50	IIIA	adeno
A14			yes	yes		62	F	Y	10	IA	adeno
A15	yes	yes	yes	yes	yes	71	F	N	3	IB	adeno
A16	yes	yes	yes	yes	yes	68	F	N	20	IB	adeno
A17	yes	yes	yes	yes	yes	65	F	Y	0	IA	adeno
A18	yes	yes	yes	yes		65	M	N	30	IB	adeno
A19	yes	yes	yes	yes	yes	70	F	N	37	IIA	adeno
A21			yes	yes		31	M	N	0	IIIA	adeno
A28	yes	yes	yes	yes	yes	64	M	N	24	IA	adeno
A29	yes	yes	yes	yes	yes	64	F	Y	0	IA	adeno
A31	yes	yes	yes	yes	yes	68	F	Y	0	IIIB	adeno
A32	yes	yes	yes	yes	yes	49	F	N	0	IB	adeno
Total # with yes	15	10	19	17	9	-	-	-	-	-	-

Data availability and clinical attributes of the Stanford NSCLC cohort. Single-cell TCR-seq was performed on 15 patients, single-cell RNA-seq was performed on 10 patients, histology was performed on tumors from 19 patients and the adjacent lung tissues from 17 patients, and 9 NSCLC patients have tumors assessed with whole-exome sequencing (yes, data available). A6*, the paired TCR CDR3α/β sequences from the tumor of patient A6 were derived by using the Chromium Single Cell Immune Profiling Solution for human T cell repertoires from the 10x Genomics. M, male; F, female; N, HLA-A*02^{-}; Y, HLA-A*02^{+};adeno, adenocarcinoma; SCC, squamous cell carcinoma.

Table S5, related to Figure 3.

Rank	Peptide seq (Naive)	#	Peptide seq (Round 1)	#	Peptide seq (Round 2)	#	Peptide seq (Round 3)	#	Peptide seq (Round 4)	#
1	SMQGLTRPPRV	43	VMRQLACSRRL	25	RLHVAPGQRRM	149	AMGGLLTQLAM	14764	AMGGLLTQLAM	70220
2	AMGGLLTQLAM	30	FLQNGRSSERM	24	RLREAAPILPM	108	EMRVASAMWGM	1205	KLGGLLTMVGV	23704
3	ALRTPRKKQTL	17	RLQSRKLPPLL	22	PMDTHLPTSVL	89	GMVEDICSTLL	712	GMVEDICSTLL	18950
4	CLTQSSQEWTL	16	TLARTHHTRRL	20	AMQERLGTRQV	88	RLHEQVPEVTL	557	EMRVASAMWGM	11431
5	KLDSANAQAIV	13	HMHRPRPSGRL	19	WLTAALPSCGV	88	HLRVKEHRHGL	469	RLHEQVPEVTL	3165
6	PMLTRSPLSRM	10	DLLVQKITRHL	18	CLPWQKTESPL	81	HMHHHNEHNRM	468	KMKMKHHTRPL	2760
7	WMRQMEPSGRL	10	RLNELRLAKGL	18	RLTRTQGSETL	78	RLHVAPGQRRM	315	HMHHHNEHNRM	1229
8	GMLASLAARQV	10	RLHKAPRPAPL	18	NMEALGHCHRL	77	PLACAKRRGGM	280	ALNLPSSPPSL	1019
9	EMTLPQTAKWL	9	DLQSTLEAWAV	17	RMEQVATARVL	73	NLKLMGIWIEM	268	KMPHRPKHKVV	987
10	WLSLAAPPPAL	9	RMSSRPRSLLL	17	RLAEPSHWIRL	67	ALNLPSSPPSL	264	HLRVKEHRHGL	968
11	RLWQRAPVTRL	9	GMRTRGPWRHL	17	RLHVRPGPRPL	67	NLRHRHPSRFL	262	HMHEHRVKGKV	841
12	GLGIAPALTDL	9	HMTGKHRTHMV	17	MMRTGPLLGLL	67	SMPKRGTQVTM	261	RLHVRPGPRPL	834
13	RMPTRRPTKRM	9	AMHRNSRWHSL	16	RMLTRSPRLAL	67	HMHEHRVKGKV	260	WLETPTTPLLL	818
14	PLAHTPPRRTL	9	ALSARLPRQAL	16	HMSRTHAPGQL	67	RLHVRPGPRPL	259	PLACAKRRGGM	573
15	TLMRLHAGVVL	9	RLHAPTHHHSL	16	MMSCPAQEPCL	67	ALREKPRLPRL	257	NLRHRHPSRFL	459
16	RMGPLALSPSM	9	ALSRARLSRPV	16	TMKTQGQETSM	66	RLPARHPPEAL	255	PLTSARKKPRM	396
17	AMPNPRVREHL	9	RLPPLPQTWPL	15	RLAHPRARQQV	65	RLPEPPPARPL	249	RLHGRPTRWNL	382
18	AMLTLTRGQQM	9	PLTPTPRPGSM	15	RMSGKPQQHPL	65	RLLAKVPQGTL	248	HMPRHRWAARV	359
19	PLPPPLPRPPM	9	PLLATARTTWV	15	NLLPWRPTKLM	63	QLRLASTPRGL	247	SMGGLLTQLAM	350
20	RMTMTARRRPV	9	ALEASWEWTGM	15	VMRTPRRPVPL	63	QMTARGRVHLL	234	RMPAAARKRGV	326
21	GLLQLMMSLAV	9	VLPALHAPGPL	15	KLAAGKQGLAM	63	RMACGQHPGPL	218	RLPARHPPEAL	314
22	RLPLEPHRQCM	8	ELARSHRAWSM	14	RLRAHQHMFRV	61	RMPAAARKRGV	217	HMRGGRHSRLM	302
23	LLASPTGVTKM	8	EMTCQLGPKPL	14	RLPKPPQVPAL	61	RMLTRSPRLAL	216	KMKSHHLRWGL	299
24	RLQVLPNSPCV	8	GLPPSAARKVL	14	NLKLMGIWIEM	60	KMHQHGQHRQL	214	PMEPSPCSTGV	293
25	KLHPNTCAKGM	8	TLKSHHHWGQL	14	PLRPPSLPTKM	60	RLHGRPTRWNL	212	KMHQHGQHRQL	286
26	TLSPSTGTVSM	8	RLIPWRTTLLL	14	VLGWRDEPGTV	60	LLPLAPPRRGV	193	HLMGTRGHRCL	282
27	RLCARMWNQSV	8	RMPPTPAPKGM	14	EMLTGAVGTPL	60	HLHSHARTPRM	190	ALREKPRLPRL	268
28	AMRPPSMATRL	8	HMPRDQNRVAL	14	PMAIHHPSSQL	59	KLGGLLTMVGV	188	HLRLRHHHREL	267
29	ALPLRPARLSL	8	PLHGRQLLRAL	14	TLQEQTARTRM	59	QLSGAHHHRAL	187	RMPRPPIPSPL	263
30	RLRWIMLRTAL	8	TLMKRPGLRGL	14	RMHARMTSLKL	59	RLHHPHQLRPM	178	RLPRPHMLPRL	260
31	CLESLCRAMQL	8	LLPPTTPPHAV	14	AMPRAPRSSWV	59	HLMGTRGHRCL	175	HMARPGPHRHL	256
32	PLPLTQRTPAV	8	RLARSPQQHSL	14	GLSGPCPQPAL	58	RMPAQRVAQAM	170	HLHPHHPPGAL	247
33	NLRQREGTRIL	7	RMDHMPWHVRL	14	RLQMSSRRHHV	58	KLNGQVSERML	169	HMHRPRPSGRL	241
34	RLPSLERWPRL	7	EMPMPPAAQPL	14	RMTPCLQAEAL	58	TLTPAQPPVLL	168	HMQHRGTHTKV	229
35	GMWARSVRASL	7	HLSKPRRRHEL	14	TMPPPGLWQAV	58	LMCTMAAASRL	168	HMPKPRTRVPL	208
36	ALRGVRRTRVL	7	ALCLASREVLM	14	RLAPPRLPHIV	57	RLPTEMGTPPL	167	HLHSHARTPRM	206
37	TLLVSTLRGCL	7	TMQHGAQQTAL	13	RLPAPHRPETV	57	MLKRPRTPRQV	165	MLFDGLPPLGV	202
38	RLSQSHRPRPL	7	TMRTCTERTPM	13	RLMWAKQEMLL	57	KMKMKHHTRPL	164	RLHVAPGQRRM	193
39	WMRVWREPVRM	7	EMAPHAMLERV	13	RLSRPPLPTGV	56	HLRLRHHHREL	162	SMPKRGTQVTM	186
40	QLSAPLAPRSL	7	NLTWLPTATRL	13	RLPMHPPALAV	56	PLSAWTATASL	162	RMPPPPPRLAL	184
41	LLRGQRLEHLL	7	RLHQPPRPLPL	13	RLPEPPGPAAV	56	LLQEEHRHPTV	162	RLHHRVVLPPL	179
42	CLLTTTPPTAL	7	RLDKVPRPGPL	13	RMARHRPGLQL	56	RMPRPPIPSPL	160	QMTARGRVHLL	177
43	QLTRWRHSKGM	7	GLQRVTGHRPL	13	RMACGQHPGPL	56	RLHKSRPWRSV	160	RLPLLPAPRLV	177
44	HLPWLPLHGRM	7	KLAPPNPRPPL	13	KLFSGKSGQVL	55	RLPARCRLGAV	160	RLPEPPGPAAV	172
45	PMAFRGWHTWM	7	HMRRPPPVRLL	13	RLPARPGPLRV	55	RMPPSLQSGCL	159	TLAPPPAPRPL	169
46	TMHGPRSRRAL	7	ELPGCAPQCLM	13	GMSMGPSQCRL	55	RLRPGSNAVLM	153	TLPLHQPPKLV	169
47	SLAWRAGAMDM	7	PLGPPRLRLPL	13	DMTSRLVRWAM	54	HMPRHRWAARV	153	HLARPPPPARL	164
48	RLLNPKGTSAM	7	SLPSAPRHGNL	13	ELRRAEELRNV	54	ALAPTRATRRV	151	RMRAFHPHTRL	164
49	RLSKSLRHTCM	7	PMPAPPLTLPL	13	QLRLASTPRGL	54	DLLPQPWARGM	149	RMRFHSPHKQL	162
50	AMMQSLPAPGM	7	VLLPPLESPPL	13	KMRRTGTLLDV	54	PMVSGEHRGAV	149	AMARPPPRPAL	161

Summary of results from each round of affinity selection on a 11mer yeast HLA-A*02 library with TCR2. Numbers (#) indicate counts of the top-50 mimotopes. Top-two mimotopes from the round 4 screen were highlighted.

Table S6, related to Figure 4.

Sample ID	Gene ID	Unique mut ID	Var class	Var type	AA var	coverage	Ref depth	Alt depth	af	dbsnp	exac	counts_cosmic	filter
A6	ABCA13	chr7:48313276:C>G	exonic	nonsense	S1338X	74	64	10	0.144	FALSE	FALSE	0	PASS
A6	ABCC11	chr16:48201528:G>T	exonic	nonsynonymous_snv	T1312K	143	119	24	0.172	FALSE	FALSE	0	PASS
A6	ADAM7	chr8:24346811:G>A	exonic	nonsynonymous_snv	D411N	71	55	16	0.233	FALSE	FALSE	0	PASS
A6	ADGRB3	chr6:69653730:G>C	exonic	nonsynonymous_snv	V347L	74	64	10	0.145	FALSE	FALSE	0	PASS
A6	AKAP9	chr7:91707139:G>A	exonic	nonsynonymous_snv	E2291K	110	96	14	0.133	FALSE	FALSE	0	PASS
A6	ALS2	chr2:202622283:C>A	exonic	nonsynonymous_snv	S438I	92	76	16	0.18	FALSE	FALSE	0	PASS
A6	ANK2	chr4:114274311:G>C	exonic	nonsynonymous_snv	D1513H	85	68	17	0.206	FALSE	FALSE	0	PASS
A6	ANKFN1	chr17:54520251:G>T	exonic	nonsynonymous_snv	W355C	86	75	11	0.136	FALSE	FALSE	0	PASS
A6	ANKLE2	chr12:133327337:C>T	exonic	nonsynonymous_snv	E247K	265	200	65	0.246	FALSE	FALSE	0	PASS
A6	ANKS1B	chr12:99640454:T>G	exonic	nonsynonymous_snv	K649Q	83	72	11	0.14	FALSE	FALSE	0	PASS
A6	ARHGEF17	chr11:73021562:A>C	exonic	nonsynonymous_snv	T627P	360	290	70	0.196	FALSE	FALSE	0	PASS
A6	ARL2	chr11:64785853:G>A	exonic	nonsynonymous_snv	G28E	318	265	53	0.168	FALSE	FALSE	0	PASS
A6	ASB9	chrX:15266932:C>T	exonic	nonsynonymous_snv	G232S	204	167	37	0.184	FALSE	FALSE	0	PASS
A6	ASIC2	chr17:32483281:G>T	exonic	nonsynonymous_snv	L91I	513	426	87	0.17	FALSE	FALSE	0	PASS
A6	ATP13A5	chr3:193048947:T>C	exonic	nonsynonymous_snv	M476V	115	71	44	0.385	FALSE	FALSE	0	PASS
A6	ATP4B	chr13:114312422:C>T	exonic	nonsynonymous_snv	R13H	685	631	54	0.079	TRUE	TRUE	0	PASS
A6	ATP7A	chrX:77296175:G>A	exonic	nonsynonymous_snv	E1249K	235	211	24	0.104	FALSE	FALSE	0	PASS
A6	AUTS2	chr7:69364300:G>A	exonic	nonsynonymous_snv	R113H	80	52	28	0.353	TRUE	TRUE	3	PASS
A6	BAI3	chr6:69653730:G>C	exonic	nonsynonymous_snv	V347L	74	64	10	0.135	FALSE	FALSE	0	PASS
A6	BCOR	chrX:39933652:G>C	exonic	nonsynonymous_snv	P316R	654	593	61	0.094	FALSE	FALSE	0	PASS
A6	BLVRA	chr7:43830961:A>T	exonic	nonsynonymous_snv	Y83F	73	61	12	0.173	FALSE	FALSE	0	PASS
A6	C1orf173	chr1:75065441:C>T	exonic	nonsynonymous_snv	R555H	67	58	9	0.134	TRUE	TRUE	1	PASS
A6	C20orf141	chr20:2795930:C>A	exonic	nonsynonymous_snv	R34S	498	421	77	0.155	FALSE	FALSE	0	PASS
A6	C20orf203	chr20:31238353:C>A	exonic	nonsynonymous_snv	A156S	742	622	120	0.162	FALSE	FALSE	0	PASS
A6	CACNA1A	chr19:13409626:C>G	exonic	nonsynonymous_snv	E941Q	697	576	121	0.174	FALSE	FALSE	0	PASS
A6	CAST	chr5:96031574:C>G	exonic	nonsynonymous_snv	S58C	54	37	17	0.32	FALSE	FALSE	0	PASS
A6	CC2D2A	chr4:15504120:G>C	exonic	nonsynonymous_snv	E106Q	232	177	55	0.239	FALSE	FALSE	0	PASS
A6	CCDC159	chr19:11460855:T>A	exonic	nonsynonymous_snv	I69N	149	135	14	0.098	FALSE	FALSE	0	PASS
A6	CCDC22	chrX:49104195:C>A	exonic	nonsynonymous_snv	A353D	1037	946	91	0.088	FALSE	FALSE	0	PASS
A6	CCNJ	chr10:97817990:G>A	exonic	nonsynonymous_snv	E371K	120	93	27	0.229	FALSE	FALSE	1	PASS
A6	CEP128	chr14:81251610:C>T	exonic	nonsynonymous_snv	E614K	109	75	34	0.315	FALSE	FALSE	0	PASS
A6	CEP95	chr17:62533725:T>C	exonic	nonsynonymous_snv	L765S	63	51	12	0.2	FALSE	FALSE	0	PASS
A6	CHIC1	chrX:72783256:G>C	exonic	nonsynonymous_snv	E46Q	338	270	68	0.203	FALSE	FALSE	0	PASS
A6	CLGN	chr4:141317335:T>C	exonic	nonsynonymous_snv	I303M	149	120	29	0.197	FALSE	FALSE	0	PASS
A6	CNBD1	chr8:88249177:T>C	exonic	nonsynonymous_snv	L203P	67	48	19	0.288	FALSE	FALSE	0	PASS
A6	COL22A1	chr8:139618637:G>C	exonic	nonsynonymous_snv	P1364R	69	55	14	0.211	FALSE	FALSE	0	PASS
A6	COL4A1	chr13:110835623:C>A	splicing	splice	G633V	151	109	42	0.278	FALSE	FALSE	0	PASS
A6	COL9A1	chr6:70965071:G>T	exonic	nonsynonymous_snv	P509H	61	55	6	0.109	FALSE	FALSE	0	PASS
A6	CTNNA2	chr2:80816447:C>A	exonic	nonsynonymous_snv	P676T	114	88	26	0.232	FALSE	FALSE	0	PASS
A6	DAW1	chr2:228767798:G>C	exonic	nonsynonymous_snv	Q192H	175	149	26	0.152	FALSE	FALSE	0	PASS
A6	DCAF8L1	chrX:27999212:T>A	exonic	nonsynonymous_snv	E80D	457	372	85	0.187	FALSE	FALSE	0	PASS
A6	DECR1	chr8:91049143:A>G	exonic	nonsynonymous_snv	K205E	58	49	9	0.166	FALSE	FALSE	0	PASS
A6	DIRAS3	chr1:68512702:C>G	exonic	nonsynonymous_snv	K93N	179	152	27	0.154	FALSE	FALSE	0	PASS
A6	DLC1	chr8:13356569:G>A	exonic	nonsynonymous_snv	R338C	89	79	10	0.12	TRUE	TRUE	2	PASS
A6	DNA2	chr10:70192032:G>T	exonic	nonsynonymous_snv	Q602K	89	78	11	0.131	FALSE	FALSE	0	PASS
A6	DNAH3	chr16:21069431:T>A	exonic	nonsynonymous_snv	Q1300H	53	46	7	0.145	FALSE	FALSE	0	PASS
A6	DNAH6	chr2:85035598:C>A	exonic	nonsynonymous_snv	L3891M	81	73	8	0.108	FALSE	FALSE	0	PASS
A6	DUSP27	chr1:167095602:G>A	exonic	nonsynonymous_snv	G412R	199	141	58	0.294	FALSE	FALSE	0	PASS
A6	DYNC1I1	chr7:95614255:G>C	exonic	nonsynonymous_snv	D254H	102	61	41	0.404	FALSE	FALSE	0	PASS
A6	EDNRB	chr13:78493532:C>A	exonic	nonsynonymous_snv	E73D	157	118	39	0.252	FALSE	FALSE	0	PASS
A6	EHMT1	chr9:140708956:A>T	exonic	nonsynonymous_snv	D1085V	346	276	70	0.203	FALSE	FALSE	0	PASS
A6	EMD	chrX:153609138:C>T	exonic	nonsynonymous_snv	S142F	295	235	60	0.205	FALSE	FALSE	0	PASS
A6	ERICH3	chr1:75065441:C>T	exonic	nonsynonymous_snv	R555H	67	58	9	0.1343	TRUE	TRUE	1	PASS
A6	FAM181B	chr11:82443751:G>A	exonic	nonsynonymous_snv	R341C	348	308	40	0.117	FALSE	FALSE	0	PASS
A6	FAT2	chr5:150886965:C>A	exonic	nonsynonymous_snv	R4089S	192	142	50	0.263	FALSE	FALSE	0	PASS
A6	FAT3	chr11:92086057:A>G	exonic	nonsynonymous_snv	N260S	130	118	12	0.097	FALSE	FALSE	0	PASS
A6	FBXO4	chr5:41927145:C>G	exonic	nonsynonymous_snv	L74V	130	116	14	0.113	FALSE	FALSE	0	PASS
A6	FGD1	chrX:54472725:G>T	exonic	nonsynonymous_snv	F901L	527	481	46	0.087	FALSE	FALSE	0	PASS
A6	FGFR2	chr10:123324084:G>A	exonic	nonsynonymous_snv	S129L	70	56	14	0.207	FALSE	FALSE	0	PASS
A6	FICD	chr12:108913075:C>A	exonic	nonsense	Y400X	249	207	42	0.171	FALSE	FALSE	0	PASS
A6	FIG4	chr6:110064446:C>T	exonic	nonsynonymous_snv	S337L	51	44	7	0.15	FALSE	FALSE	0	PASS
A6	FLT4	chr5:180041175:C>T	exonic	nonsynonymous_snv	R1075Q	682	543	139	0.204	FALSE	FALSE	2	PASS
A6	FPR1	chr19:52249356:G>T	exonic	nonsynonymous_snv	P298T	235	177	58	0.249	FALSE	FALSE	0	PASS
A6	FREM1	chr9:14859371:G>C	exonic	nonsynonymous_snv	F147L	184	156	28	0.156	TRUE	TRUE	0	PASS
A6	FRK	chr6:116325135:G>C	exonic	nonsense	S124X	69	57	12	0.181	FALSE	FALSE	0	PASS
A6	GALNT13	chr2:154996951:C>T	exonic	nonsense	Q82X	82	59	23	0.285	FALSE	FALSE	0	PASS
A6	GLB1L	chr2:220107905:C>G	exonic	nonsynonymous_snv	L68F	193	158	35	0.184	FALSE	FALSE	0	PASS
A6	GNA12	chr7:2883750:C>T	exonic	nonsynonymous_snv	E16K	40	24	16	0.405	FALSE	FALSE	0	PASS
A6	GOLGA6L2	chr15:23686407:C>A	exonic	nonsynonymous_snv	R405S	737	644	93	0.127	FALSE	FALSE	0	PASS

A6	GOLGB1	chr3:121414947:C>T	exonic	nonsynonymous_snv	E1470K	81	56	25	0.312	FALSE	FALSE	0	PASS
A6	GPC3	chrX:132795781:C>G	exonic	nonsynonymous_snv	D487H	80	64	16	0.207	FALSE	FALSE	0	PASS
A6	GRM3	chr7:86416222:G>T	exonic	nonsynonymous_snv	V372F	482	422	60	0.125	FALSE	FALSE	0	PASS
A6	GSK3B	chr3:119631590:C>G	exonic	nonsynonymous_snv	E226Q	48	43	5	0.119	FALSE	FALSE	0	PASS
A6	HMGCS1	chr5:43298731:C>T	exonic	nonsynonymous_snv	E113K	108	93	15	0.144	FALSE	FALSE	0	PASS
A6	HPN	chr19:35556161:C>G	exonic	nonsynonymous_snv	I273M	232	143	89	0.385	FALSE	FALSE	0	PASS
A6	HTATSF1	chrX:135593097:G>C	exonic	nonsynonymous_snv	R398T	178	141	37	0.21	FALSE	FALSE	0	PASS
A6	IFT140	chr16:1634385:C>G	exonic	nonsynonymous_snv	V398L	209	173	36	0.175	TRUE	FALSE	0	PASS
A6	IKBIP	chr12:99038439:C>G	exonic	nonsynonymous_snv	G14A	1117	887	230	0.206	FALSE	FALSE	0	PASS
A6	ITPR3	chr6:33655009:G>A	exonic	nonsynonymous_snv	V2028I	293	240	53	0.183	TRUE	TRUE	0	PASS
A6	KAT8	chr16:31141434:G>C	exonic	nonsynonymous_snv	E290Q	228	204	24	0.109	FALSE	FALSE	1	PASS
A6	KIAA1191	chr5:175774788:G>A	exonic	nonsense	R245X	130	107	23	0.182	FALSE	FALSE	1	PASS
A6	KIAA1324L	chr7:86554885:G>A	exonic	nonsynonymous_snv	S339F	79	69	10	0.135	FALSE	FALSE	1	PASS
A6	KIAA1524	chr3:108300342:C>G	exonic	nonsynonymous_snv	E157Q	93	61	32	0.347	FALSE	FALSE	0	PASS
A6	KIF20A	chr5:137518944:G>A	exonic	nonsynonymous_snv	E307K	101	83	18	0.185	FALSE	FALSE	0	PASS
A6	KIF25	chr6:168431475:C>G	exonic	nonsynonymous_snv	Q39E	108	83	25	0.236	TRUE	TRUE	0	PASS
A6	KIF26B	chr1:245850140:G>A	exonic	nonsynonymous_snv	M1285I	548	495	53	0.097	FALSE	FALSE	0	PASS
A6	KIF4A	chrX:69561692:C>G	exonic	nonsynonymous_snv	Q393E	94	76	18	0.196	FALSE	FALSE	1	PASS
A6	KLHL15	chrX:24024710:G>T	exonic	nonsynonymous_snv	T34N	141	111	30	0.216	FALSE	FALSE	0	PASS
A6	KLRG1	chr12:9162105:A>T	exonic	nonsynonymous_snv	H102L	103	80	23	0.228	FALSE	FALSE	0	PASS
A6	KNTC1	chr12:123019308:C>A	exonic	nonsense	S76X	92	82	10	0.116	FALSE	FALSE	0	PASS
A6	LDOC1	chrX:140270961:G>T	exonic	nonsynonymous_snv	F82L	591	470	121	0.205	FALSE	FALSE	0	PASS
A6	LRTM1	chr3:54958718:T>A	exonic	nonsense	K178X	91	62	29	0.324	TRUE	TRUE	0	PASS
A6	LYST	chr1:235894365:T>G	exonic	nonsynonymous_snv	K2972Q	169	132	37	0.221	FALSE	FALSE	0	PASS
A6	MAGEA1	chrX:152482674:G>T	exonic	nonsynonymous_snv	L113M	313	255	58	0.187	FALSE	FALSE	0	PASS
A6	MAGEA10	chrX:151303932:G>T	exonic	nonsynonymous_snv	S54Y	254	216	38	0.152	FALSE	FALSE	0	PASS
A6	MAGI1	chr3:65342735:C>A	exonic	nonsynonymous_snv	R1236L	261	213	48	0.186	FALSE	FALSE	0	PASS
A6	MAP2	chr2:210594676:G>T	exonic	nonsynonymous_snv	G1753V	55	48	7	0.139	FALSE	FALSE	0	PASS
A6	MAP3K4	chr6:161514830:G>T	exonic	nonsynonymous_snv	C578F	72	62	10	0.149	FALSE	FALSE	0	PASS
A6	MGAT5B	chr17:74922812:C>T	exonic	nonsynonymous_snv	P431S	292	263	29	0.101	TRUE	TRUE	4	PASS
A6	MORF4L1	chr15:79172879:A>G	exonic	nonsynonymous_snv	K38R	50	41	9	0.192	FALSE	FALSE	0	PASS
A6	MROH2B	chr5:41042265:C>T	exonic	nonsynonymous_snv	D628N	118	99	19	0.166	FALSE	FALSE	0	PASS
A6	MS4A18	chr11:60506423:G>T	exonic	nonsynonymous_snv	A193S	129	117	12	0.098	FALSE	FALSE	0	PASS
A6	MTMR3	chr22:30384487:G>C	exonic	nonsynonymous_snv	E77Q	94	79	15	0.166	FALSE	FALSE	0	PASS
A6	MTTP	chr4:100503214:C>G	exonic	nonsynonymous_snv	P72A	70	51	19	0.277	FALSE	FALSE	0	PASS
A6	MTUS2	chr13:30077281:G>A	exonic	nonsynonymous_snv	V1360I	244	196	48	0.199	TRUE	TRUE	1	PASS
A6	MYEF2	chr15:48450201:G>A	exonic	nonsynonymous_snv	P325L	55	42	13	0.244	TRUE	TRUE	0	PASS
A6	NCAN	chr19:19338481:G>T	exonic	nonsynonymous_snv	L684F	339	307	32	0.095	FALSE	FALSE	0	PASS
A6	NDUFB9	chr8:125551440:G>T	exonic	nonsynonymous_snv	A5S	440	401	39	0.089	FALSE	FALSE	0	PASS
A6	NECAB1	chr8:91953091:C>A	exonic	nonsense	Y275X	152	124	28	0.188	FALSE	FALSE	0	PASS
A6	NFAT5	chr16:69718837:C>T	exonic	nonsynonymous_snv	P486S	69	57	12	0.183	TRUE	TRUE	0	PASS
A6	NFE2L2	chr2:178096280:T>G	exonic	nonsynonymous_snv	S351R	142	112	30	0.215	FALSE	FALSE	0	PASS
A6	NHLRC4	chr16:618291:A>G	exonic	nonsynonymous_snv	I82V	583	470	113	0.194	FALSE	FALSE	0	PASS
A6	NLRP4	chr19:56369450:G>T	exonic	nonsynonymous_snv	D231Y	200	145	55	0.277	FALSE	FALSE	0	PASS
A6	NMUR1	chr2:232389993:C>A	exonic	nonsynonymous_snv	G348C	403	327	76	0.19	FALSE	FALSE	0	PASS
A6	NOTCH2	chr1:120497715:C>T	exonic	nonsynonymous_snv	E723K	187	158	29	0.158	TRUE	TRUE	2	PASS
A6	NR0B1	chrX:30327047:A>G	exonic	nonsynonymous_snv	I145T	959	872	87	0.091	FALSE	FALSE	0	PASS
A6	NRP2	chr2:206562303:G>T	exonic	nonsynonymous_snv	A37S	236	216	20	0.087	FALSE	FALSE	0	PASS
A6	NRXN3	chr14:78709656:G>T	exonic	nonsynonymous_snv	D74Y	222	173	49	0.222	FALSE	FALSE	0	PASS
A6	OBSCN	chr1:228560380:G>A	exonic	nonsynonymous_snv	E8258K	548	445	103	0.188	TRUE	TRUE	0	PASS
A6	PCDHB15	chr5:140625549:G>C	exonic	nonsynonymous_snv	E135Q	226	165	61	0.272	FALSE	FALSE	0	PASS
A6	PCDHGB2	chr5:140741957:A>T	exonic	nonsynonymous_snv	Y752F	315	229	86	0.274	FALSE	FALSE	0	PASS
A6	PCDHGB7	chr5:140798837:A>G	exonic	nonsynonymous_snv	I471V	466	377	89	0.192	FALSE	FALSE	0	PASS
A6	PDE5A	chr4:120488257:C>T	exonic	nonsynonymous_snv	G240S	54	41	13	0.249	TRUE	TRUE	0	PASS
A6	PDGFRA	chr4:55138618:C>T	exonic	nonsynonymous_snv	T457M	203	180	23	0.116	TRUE	TRUE	2	PASS
A6	PER1	chr17:8045134:G>A	exonic	nonsynonymous_snv	L1197F	227	195	32	0.143	FALSE	FALSE	0	PASS
A6	PGAM4	chrX:77225005:G>C	exonic	nonsynonymous_snv	A44G	384	316	68	0.176	FALSE	FALSE	0	PASS
A6	PHKA1	chrX:71932728:C>G	exonic	nonsynonymous_snv	V44L	242	209	33	0.138	FALSE	FALSE	0	PASS
A6	PIEZO2	chr18:10789214:G>C	exonic	nonsynonymous_snv	L678V	276	177	99	0.359	FALSE	FALSE	0	PASS
A6	PKN2	chr1:89271206:A>G	exonic	nonsynonymous_snv	M510V	74	61	13	0.184	FALSE	FALSE	0	PASS
A6	PLA2G4A	chr1:186916078:A>G	exonic	nonsynonymous_snv	M417V	39	25	14	0.366	FALSE	FALSE	0	PASS
A6	PLCH1	chr3:155199800:C>G	exonic	nonsynonymous_snv	D1338H	244	199	45	0.186	FALSE	FALSE	0	PASS
A6	PLXNA2	chr1:208219335:G>T	exonic	nonsynonymous_snv	S1128Y	234	214	20	0.088	FALSE	FALSE	1	PASS
A6	PPP1R13L	chr19:45885927:T>C	exonic	nonsynonymous_snv	Y769C	547	375	172	0.315	TRUE	TRUE	0	PASS
A6	PPP2CB	chr8:30655241:C>G	exonic	nonsynonymous_snv	L114F	78	62	16	0.212	FALSE	FALSE	0	PASS
A6	PRKCB	chr16:24192133:A>G	exonic	nonsynonymous_snv	M473V	57	50	7	0.135	FALSE	FALSE	0	PASS
A6	PRPS2	chrX:12837682:G>T	exonic	nonsynonymous_snv	R196M	254	198	56	0.222	FALSE	FALSE	0	PASS
A6	PRR23A	chr3:138724393:C>A	exonic	nonsynonymous_snv	V240L	783	670	113	0.145	FALSE	FALSE	0	PASS
A6	PRSS56	chr2:233388226:G>T	exonic	nonsynonymous_snv	G317V	567	441	126	0.222	FALSE	FALSE	0	PASS
A6	PTPRF	chr1:44084976:C>T	exonic	nonsynonymous_snv	T1285I	91	80	11	0.128	FALSE	FALSE	0	PASS
A6	PTPRO	chr12:15661514:G>A	exonic	nonsynonymous_snv	G426E	170	151	19	0.115	FALSE	FALSE	0	PASS
A6	QSER1	chr11:32956207:G>A	exonic	nonsynonymous_snv	E1006K	104	81	23	0.225	FALSE	FALSE	0	PASS
A6	RANBP17	chr5:170725797:G>A	exonic	nonsynonymous_snv	D1068N	85	59	26	0.31	FALSE	FALSE	0	PASS
A6	RBFOX3	chr17:77102861:C>G	exonic	nonsynonymous_snv	E78Q	583	465	118	0.203	FALSE	FALSE	0	PASS
A6	ROBO1	chr3:78685196:C>G	exonic	nonsynonymous_snv	E1034Q	93	63	30	0.326	FALSE	FALSE	0	PASS
A6	RORC	chr1:151787559:C>T	exonic	nonsynonymous_snv	R214K	223	142	81	0.365	FALSE	FALSE	0	PASS

A6	RP11-321N4.5	chr6:86322638:C>A	splicing	splice	G85G	68	57	11	0.162	FALSE	FALSE	0	PASS
A6	RP11-399J13.3	chr11:64785853:G>A	exonic	nonsynonymous_snv	G28E	324	271	53	0.164	FALSE	FALSE	0	PASS
A6	RTCB	chr22:32792234:C>T	exonic	nonsynonymous_snv	A273T	77	65	12	0.164	FALSE	FALSE	0	PASS
A6	RTP2	chr3:187416515:T>C	exonic	nonsynonymous_snv	H150R	883	685	198	0.225	FALSE	FALSE	0	PASS
A6	SACS	chr13:23911873:C>T	exonic	nonsynonymous_snv	E2048K	107	92	15	0.146	FALSE	FALSE	1	PASS
A6	SC5D	chr11:121177887:T>C	exonic	nonsynonymous_snv	L189S	116	102	14	0.126	TRUE	TRUE	0	PASS
A6	SHISA8	chr22:42306502:C>A	exonic	nonsynonymous_snv	G241C	530	461	69	0.131	FALSE	FALSE	0	PASS
A6	SLC10A2	chr13:103703691:A>T	exonic	nonsynonymous_snv	L226Q	132	83	49	0.373	TRUE	TRUE	0	PASS
A6	SLC12A8	chr3:124854600:C>A	exonic	nonsense	E217X	192	143	49	0.257	TRUE	TRUE	0	PASS
A6	SLC14A1	chr18:43319130:G>T	exonic	nonsynonymous_snv	L222F	93	67	26	0.284	FALSE	FALSE	0	PASS
A6	SLC16A2	chrX:73740853:G>C	exonic	nonsynonymous_snv	M153I	188	141	47	0.252	FALSE	FALSE	0	PASS
A6	SLC2A13	chr12:40441855:C>G	exonic	nonsynonymous_snv	W238C	74	64	10	0.143	FALSE	FALSE	1	PASS
A6	SLC40A1	chr2:190428865:T>A	exonic	nonsynonymous_snv	T283S	198	179	19	0.099	FALSE	FALSE	0	PASS
A6	SLC4A10	chr2:162627561:G>C	exonic	nonsynonymous_snv	E54Q	35	29	6	0.188	FALSE	FALSE	0	PASS
A6	SLC5A7	chr2:108627285:G>C	exonic	nonsynonymous_snv	E571Q	61	49	12	0.206	FALSE	FALSE	0	PASS
A6	SORCS1	chr10:108536359:T>C	exonic	nonsynonymous_snv	Y273C	66	59	7	0.118	TRUE	TRUE	0	PASS
A6	SPANXN1	chrX:144337210:G>C	exonic	nonsynonymous_snv	R32T	131	107	24	0.187	FALSE	FALSE	0	PASS
A6	SPEN	chr1:16260921:C>T	exonic	nonsynonymous_snv	A2729V	209	174	35	0.17	TRUE	TRUE	0	PASS
A6	SRRM1	chr1:24981357:C>T	exonic	nonsynonymous_snv	S351L	89	81	8	0.098	FALSE	FALSE	2	PASS
A6	ST3GAL4	chr11:126277484:G>T	exonic	nonsynonymous_snv	R120L	398	356	42	0.106	FALSE	FALSE	0	PASS
A6	SUGP1	chr19:19389597:C>T	exonic	nonsynonymous_snv	E513K	215	175	40	0.189	FALSE	FALSE	0	PASS
A6	SYNCRIP	chr6:86322638:C>A	exonic	nonsense	G551X	68	57	11	0.17	FALSE	FALSE	0	PASS
A6	SYNE1	chr6:152675975:T>C	exonic	nonsynonymous_snv	Y3582C	126	111	15	0.125	FALSE	FALSE	0	PASS
A6	TACR3	chr4:104512737:C>A	exonic	nonsynonymous_snv	W331L	82	66	16	0.202	FALSE	FALSE	0	PASS
A6	TAS2R13	chr12:11061142:C>G	exonic	nonsynonymous_snv	W252C	100	68	32	0.323	FALSE	FALSE	0	PASS
A6	TBC1D23	chr3:100038044:C>T	exonic	nonsynonymous_snv	P607S	115	104	11	0.099	FALSE	FALSE	0	PASS
A6	TBX1	chr22:19753930:G>T	exonic	nonsynonymous_snv	R343L	297	254	43	0.147	FALSE	FALSE	0	PASS
A6	TECTA	chr11:121028698:C>T	exonic	nonsynonymous_snv	S1485F	359	288	71	0.199	FALSE	FALSE	1	PASS
A6	TMEM200C	chr18:5890672:T>A	exonic	nonsynonymous_snv	Y464F	428	274	154	0.361	FALSE	FALSE	0	PASS
A6	TMEM239	chr20:2795930:C>A	exonic	nonsynonymous_snv	R34S	502	424	78	0.156	FALSE	FALSE	0	PASS
A6	TP53	chr17:7577082:C>A	exonic	nonsense	E247X	109	90	19	0.18	FALSE	FALSE	37	PASS
A6	TPO	chr2:1499952:G>A	exonic	nonsynonymous_snv	R733K	542	493	49	0.091	FALSE	FALSE	0	PASS
A6	TRPM8	chr2:234839319:G>A	exonic	nonsynonymous_snv	V42M	44	32	12	0.281	FALSE	FALSE	0	PASS
A6	TRRAP	chr7:98602936:G>A	exonic	nonsynonymous_snv	R3559K	450	378	72	0.16	FALSE	FALSE	0	PASS
A6	TTN	chr2:179456135:G>T	exonic	nonsynonymous_snv	P20106H	125	94	31	0.252	FALSE	FALSE	1	PASS
A6	TUBGCP6	chr22:50659585:G>A	exonic	nonsynonymous_snv	S1068L	696	590	106	0.153	FALSE	FALSE	0	PASS
A6	URAD	chr13:28552584:C>A	exonic	nonsense	E61X	148	121	27	0.186	FALSE	FALSE	0	PASS
A6	USH2A	chr1:216595521:G>T	exonic	nonsynonymous_snv	P53Q	141	114	27	0.194	FALSE	FALSE	0	PASS
A6	UTP20	chr12:101767513:G>C	exonic	nonsynonymous_snv	D2367H	138	124	14	0.106	TRUE	TRUE	0	PASS
A6	VAX1	chr10:118896040:G>T	exonic	nonsense	Y124X	465	377	88	0.19	TRUE	TRUE	0	PASS
A6	VMA21	chrX:150565812:C>T	exonic	nonsynonymous_snv	A11V	264	223	41	0.157	FALSE	FALSE	0	PASS
A6	VPS13C	chr15:62170909:C>T	exonic	nonsynonymous_snv	E3347K	40	27	13	0.332	TRUE	FALSE	0	PASS
A6	VWA5A	chr11:123988993:G>T	exonic	nonsynonymous_snv	G115V	128	97	31	0.246	TRUE	TRUE	0	PASS
A6	WDR24	chr16:735301:C>A	exonic	nonsynonymous_snv	V659F	884	695	189	0.214	FALSE	FALSE	0	PASS
A6	XIRP2	chr2:167992549:G>T	exonic	nonsynonymous_snv	S180I	64	53	11	0.181	FALSE	FALSE	0	PASS
A6	XKR7	chr20:30584398:C>A	exonic	nonsynonymous_snv	P293Q	660	564	96	0.146	FALSE	FALSE	0	PASS
A6	YJEFN3	chr19:19640173:G>T	exonic	nonsynonymous_snv	R20S	707	577	130	0.184	FALSE	FALSE	0	PASS
A6	ZIC1	chr3:147131169:A>T	exonic	nonsynonymous_snv	Q392L	297	234	63	0.213	FALSE	FALSE	0	PASS
A6	ZNF197	chr3:44671013:G>C	exonic	nonsynonymous_snv	D123H	139	106	33	0.237	FALSE	FALSE	0	PASS
A6	ZNF197;ZNF660-ZNF197	chr3:44671013:G>C	exonic	nonsynonymous_snv	D123H	138	105	33	0.242	FALSE	FALSE	0	PASS
A6	ZNF367	chr9:99180195:G>C	exonic	nonsynonymous_snv	I40M	298	241	57	0.193	FALSE	FALSE	0	PASS
A6	ZNF383	chr19:37726574:A>G	exonic	nonsynonymous_snv	M45V	162	89	73	0.451	TRUE	TRUE	0	PASS
A6	ZNF41	chrX:47307429:T>A	exonic	nonsynonymous_snv	E580D	99	85	14	0.148	FALSE	FALSE	0	PASS
A6	ZNF768	chr16:30536686:G>A	exonic	nonsynonymous_snv	R259W	327	286	41	0.127	FALSE	FALSE	1	PASS

Exome-seq result of the resected tumor from Stanford NSCLC patient A6.